General Disclaimer

One or more of the Following Statements may affect this Document

- This document has been reproduced from the best copy furnished by the organizational source. It is being released in the interest of making available as much information as possible.

- This document may contain data, which exceeds the sheet parameters. It was furnished in this condition by the organizational source and is the best copy available.

- This document may contain tone-on-tone or color graphs, charts and/or pictures, which have been reproduced in black and white.

- This document is paginated as submitted by the original source.

- Portions of this document are not fully legible due to the historical nature of some of the material. However, it is the best reproduction available from the original submission.

Statistical Analysis

OF A

PLANETARY RADAR ALTIMETER MEASURING UNIT

WILLIAM D. STANLEY

WAYNE R. POWELL

Prepared for

LANGLEY RESEARCH CENTER

NASA, HAMPTON, VIRGINIA

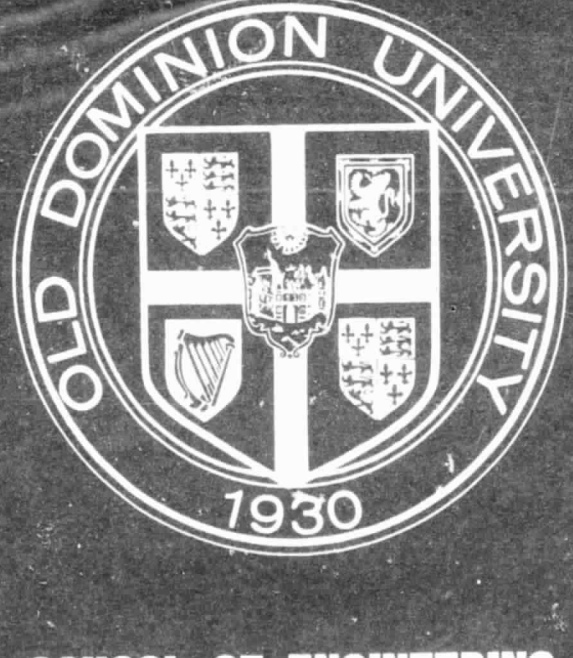

SCHOOL OF ENGINEERING

OLD DOMINION UNIVERSITY

NORFOLK, VIRGINIA

SEPTEMBER, 1969 TECHNICAL REPORT NO. 69-101

STATISTICAL ANALYSIS
OF A
PLANETARY RADAR ALTIMETER
MEASURING UNIT

WILLIAM D. STANLEY

WAYNE R. POWELL

PREPARED FOR

LANGLEY RESEARCH CENTER

NASA, HAMPTON, VIRGINIA

SCHOOL OF ENGINEERING

OLD DOMINION UNIVERSITY

NORFOLK, VIRGINIA

SEPTEMBER, 1969 TECHNICAL REPORT NO. 69-101

PREFACE

The work reported herein was performed by the School of Engineering of Old Dominion University for the Langley Research Center, NASA, Hampton, Virginia, as the first phase of NASA Grant #47-003-015. The principal investigator for this grant was Dr. William D. Stanley of ODU, and the period of performance was from 1 February 1969 to 31 May 1969.

Acknowledgment is hereby given to Mr. W. T. Bundick of the Flight Instrumentation Division of NASA, who assisted in the mathematical formulation of the problem and provided experimental data for comparison.

TABLE OF CONTENTS

LIST OF ILLUSTRATIONS

ABSTRACT

The statistical analysis of the altitude measuring unit of a proposed light-weight AM-CW radar altimeter is presented. The mathematical model was obtained by assuming a finite number of statistically independent samples during a period, which is related to the required transmission bandwidth. The mathematical model was readily implemented on an IBM 1130 computer.

The analysis was first performed with Gaussian statistics in order to verify the validity of the model by comparison with experimental data taken under similar conditions. The results obtained showed excellent correlation between experimental and computer results. The analysis was then performed with Rayleigh statistics in order to predict the expected performance of an RF unit with a linear envelope detector.

A compilation of data indicating the expected performance of the unit under a wide range of operating parameters is presented.

I. INTRODUCTION

A lightweight AM-CW radar altimeter for use in space applications is currently undergoing development in the Telemetry Techniques Section of the Flight Instrumentation Division (FID) at Langley Research Center (LRC). The proposed altimeter incorporates straight-forward design concepts and principles of operation, and it will be capable of utilizing integrated circuits quite extensively. The end result should be a radar altimeter of reasonable accuracy, but with the desirable properties of being light-weight and small in size, thus, making it suitable for certain space missions in which weight and size are at a premium.

The basic pulsed sinusoidal or AM-CW type of system was chosen for this purpose. A block diagram of the proposed system is shown in Fig. 1. Further details of the Altitude Measuring Unit (AMU) are shown in Fig. 2.

Operation of the system can be explained by means of the video-basis waveforms shown in Fig. 3. The master timer circuit sets the bistable multivibrator (flip-flop) in the "on" state at the instant at which the outgoing pulse is transmitted. In order to distinguish between the proper return echo and extraneous noise, the Schmidt trigger or comparator circuit produces an output pulse only if the signal at the input exceeds the threshold level A. In the ideal case background noise alone would not be

sufficient to exceed the threshold level, but the signal plus noise would be sufficient. In this latter case, the return signal at T_r would cause the Schmidt trigger to generate a pulse, which in turn is applied to the reset terminal of the flip-flop. The state of the flip-flop would then be changed back to the "off" state. The output of the flip-flop will thus be a square-wave whose duty cycle is directly proportional to the altitude, within the bound imposed by the maximum unambigious altitude (corresponding to the total period T_o). Since the average value of a square-wave is directly proportional to the duty cycle, a simple averaging circuit (e.g. low-pass filter) connected to the output of the flip-flop will produce a dc voltage proportional to the altitude.

The preceding discussion has assumed that noise alone would not exceed the threshold level, but signal plus noise would exceed it. Unless the signal-to-noise ratio (SNR) could be made to become infinitely large, this ideal situation would never quite exist. The presence of the noise will result in some false triggerings and in the suppression of some true signals for a finite SNR. Such undesirable effects will result in deviations from the correct mean value of a given altitude measurement.

The purpose of this study was to investigate the expected range of accuracy of the proposed Altitude Measuring Unit under a wide variety of signal-to-noise

ratios and threshold level settings. The results of the investigation should assist in determining the following requirements: (1) range of the signal-to-noise ratio required for a given accuracy and (2) optimum threshold setting to minimize error.

In the actual radar altimeter, a linear envelope detector will probably be employed. In this case, it is known{1}, {2} that the detected noise alone has Rayleigh amplitude distribution and the detected signal plus noise has a modified Rayleigh amplitude distribution. Thus, an error analysis employing these statistics would be of significant importance for the final application.

On the other hand, a prototype model of the AMU has been constructed at LRC and tested with a noise generator possessing Gaussian statistics as shown in Fig. 4. It was decided then to employ Gaussian statistics as a first step in the present analysis for two reasons: (1) Some of the analytical data could be compared with some of the experimental data as a means of checking the validity of the analytical approach. (2) Although not directly applicable to the present altimeter design, the results of the study employing Gaussian statistics would be a subject of interest in its own right, and it could be applicable to other situations.

In view of this discussion, the analysis was performed for the system employing Gaussian statistics, and it

was then repeated with the Rayleigh statistics. The details of the analysis will be presented in this report, and data providing the expected readings of the altimeter under a wide variety of conditions as predicted by computer calculations will be given.

II. STATISTICAL FORMULATION

There are four separate possible ways in which the signal and/or noise may affect the AMU during a given period. Descriptions of these possibilities are illustrated in Fig. 5, and brief explanations are given below.

Case 1

The noise alone does not exceed the threshold level in the time interval before the pulse arrives, but the return pulse does exceed the threshold level. The flip-flop trigger gates are connected so that no further change in state can occur between the time that the output is returned to the "zero" state and the time that the master timer begins the next cycle. Thus, it is immaterial whether or not noise exceeds the threshold level during the time interval after the signal has resulted in proper triggering. This case represents the desirable outcome, and it will be called a true reading.

Case 2

A noise component may exceed the threshold level in the time interval before the pulse arrives resulting in an early false alarm. This condition would result in a reading lower than the correct altitude for the given cycle. For a given SNR, the problem of early false alarms is more serious at higher altitudes since there will be much more opportunity for the noise to exceed the

threshold as the return pulse delay increases.

Case 3

It is possible that the noise alone will not exceed the threshold level before the pulse arrives, but a negative-going noise spike can suppress the signal at the instant that the signal arrives, thus, resulting in a failure to turn off the flip-flop at the proper time. This condition will be referred to as a miss. Finally, it is then possible that the noise will later exceed the threshold level in the time interval after the pulse arrives, but before the end of the period. This condition will be referred to as a late false alarm.

Case 4

The last possible outcome is equivalent to Case 3 up through and including the suppression of the signal by the noise. However, in this last case, the noise fails to exceed the threshold level in the interval following the return pulse. This means that for the given cycle, the reading will be the very maximum unambigious altitude reading corresponding to the period T_o. This possibility will be called a complete miss.

The general form of the mathematical analysis will now be developed. In later sections, some of the terms will be expanded in both the Gaussian and Rayleigh forms respectively. However, the basic analysis of this section

is applicable to both cases.

The assumptions employed in the analysis are:

(a) As a result of the bandlimiting action of the IF amplifier, the input noise to the AMU may be considered to consist of a finite number of statistically independent samples during a given period.

(b) The return pulse will be approximated as an ideal square pulse for the purpose of the statistical analysis. This assumption results in a simple shift of the statistical distribution of the noise about the level of the signal when the signal is present.

(c) The matched "optimum" equivalent low-pass bandwidth B will be chosen as

$$B = \frac{.5}{\tau} \tag{1}$$

where τ is the pulse width. This approximation is discussed in more detail in such radar texts as Skolnik {1} and Barton {2}.

In determining the number of independent samples during a period, a basic theorem of sampled-data theory was employed. This theorem, interpreted in the light of the present development, implies that the number of independent samples (j) is related to the bandwidth B and the time interval T_o by the relationship

$$j = \{2BT_o\} \tag{2}$$

where the brackets denote the process of quantization to the nearest integer. From this point on, this quantization process will be understood in similar expressions.

The assumption of (2) was employed in most of this analysis. On the other hand, there is some question regarding the exact equivalence of an "independent sample" in the sampled-data context and an "independent sample" in the statistical context. Furthermore, in the calculations of radar false alarm rates, e.g. Skolnik {1} and Barton {2}, the assumption is often made that the number of independent samples is one-half the value given by (2), i.e. BT_o. The matter is further complicated by the choice of an appropriate definition of the equivalent bandwidth B with a practical filter.

The dilemma posed by the preceding paragraph is probably a topic worthy of an investigation in its own right. As previously stated, the value of j corresponding to (2) was employed in most of this investigation. The only departure from this assumption was one set of computations performed using $j = BT_o$. The differences in results between the two different assumptions will be discussed later.

Returning to the assumption of (2), if (1) is substituted in (2), there results

$$j = \frac{T_o}{\tau} \qquad (3)$$

Assume that the pulse returns at a time T_r measured from

the beginning of a cycle. An integer i will be defined as

$$i = \frac{T_r}{\tau} \tag{4}$$

Thus, i represents the proper interval at which triggering should occur, and j represents the interval corresponding to the very maximum unambigious altitude.

Let n represent a random discrete variable describing the particular interval at which triggering occurs, and let P(n) represent the discrete probability density function describing the relative probability that triggering occurs in the nth interval. Let p represent the probability that a sample of noise alone will <u>not</u> exceed the threshold, and let q represent the probability that a sample of signal plus noise will exceed the threshold. With reference to the four cases discussed at the beginning of this section, P(n) can be described in a piecewise fashion as

$$\begin{aligned} P(n) &= p^{n-1}(1-p) && 1 \leq n < i && \text{(Case 2)} \\ &= p^{i-1}q && n=i && \text{(Case 1)} \\ &= p^{n-2}(1-q)(i-p) && i<n<j && \text{(Case 3)} \\ &= p^{j-2}(1-q) && n=j && \text{(Case 4)} \end{aligned} \tag{5}$$

In manipulating these and other expressions later in this report, certain summation formulas were derived for convenience. These formulas are tabulated in the Appendix. Using formula (A1) it can be verified that

$$\sum_{1}^{j} P(n) = 1 \tag{6}$$

The mean or expected value of the triggering interval $\bar{n}$ is given by the basic statistical formulation

$$\bar{n} = \sum_{1}^{j} nP(n)$$

$$= \sum_{1}^{i-1} np^{n-1}(1-p) + ip^{i-1}q \qquad (7)$$

$$+ \sum_{i+1}^{j-1} np^{n-2}(1-q)(1-p) + jp^{j-2}(1-q)$$

By means of the summation formulas of the Appendix, this series of terms may be manipulated to yield the following closed-form expression:

$$\bar{n} = \frac{1-p^i + (1-q)(p^{i-1} - p^{j-1})}{1-p} \qquad (8)$$

Within the quantizing error corresponding to a pulse width τ, the ideal value of $\bar{n}$ should be equal to i. In the presentation of data later in the report, the value of $\bar{n}$ is normalized with respect to i, or the ratio $\bar{n}/i$ is actually plotted. This quantity is labeled on the curves as "ratio of indicated to actual altitude."

III. GAUSSIAN STATISTICS

The development of the preceding section will now be expanded with Gaussian statistics. Let $p_1(v)$ represent the probability density function of a random Gaussian noise voltage, and let $p_2(v)$ represent the probability density function of the noise voltage plus an ideal square-pulse of amplitude E. These functions may be expressed as

$$p_1(v) = \frac{1}{\sqrt{2\pi}\sigma} \varepsilon^{-\frac{v^2}{2\sigma^2}} \qquad -\infty<v<\infty \qquad (9)$$

$$p_2(v) = \frac{1}{\sqrt{2\pi}\sigma} \varepsilon^{-\frac{(v-E)^2}{2\sigma^2}} \qquad -\infty<v<\infty \qquad (10)$$

where σ is the root-mean-square (RMS) value of the noise.

Let A represent the threshold level. The quantities p and q of the preceding section may be expressed as

$$p = \int_{-\infty}^{A} p_1(v)dv \qquad (11)$$

$$q = \int_{A}^{\infty} p_2(v)dv \qquad (12)$$

Note that for Gaussian statistics

$$p_2(v) = p_1(v-E) \qquad (13)$$

A change in variables in conjunction with (13) and recognition of the symmetry of the Gaussian function results in the following alternate form for q:

$$q = \int_{-\infty}^{E-A} p_1(v)\,dv \qquad (14)$$

Thus, both p and q may be evaluated from integrating the zero-mean process of (9) with different limits chosen for the two quantities.

The signal-to-noise ratio s will be defined as the ratio of peak signal voltage to RMS noise voltage; i.e.

$$s = \frac{E}{\sigma} \qquad (15)$$

In keeping with common convention, this quantity is often expressed in decibels (dB) as

$$s(dB) = 20 \log_{10} \frac{E}{\sigma} \qquad (16)$$

As a final convenience in evaluating the integrals, the voltage scale may be normalized with respect to the noise voltage. Let

$$x = \frac{v}{\sigma} \qquad (17)$$

After substitution of (15) and (17) in (11) and (14), and subsequent manipulation, the following forms can be obtained:

$$p = \int_{-\infty}^{as} \frac{1}{\sqrt{2\pi}} \varepsilon^{\frac{-x^2}{2}}\,dx \qquad (18)$$

$$q = \int_{-\infty}^{(1-a)s} \frac{1}{\sqrt{2\pi}} \varepsilon^{-\frac{x^2}{2}} \, dx \qquad (19)$$

The quantity a is a relative threshold level normalized with respect to the signal level E; i.e.

$$a = \frac{A}{E} \qquad (20)$$

The forms given by (18) and (19) were used in the numerical evaluation to be described later.

IV. RAYLEIGH STATISTICS

A development will now be made employing statistics appropriate to an actual RF signal followed by linear detection. It can be shown {1}, {2} that passage of relatively narrow-band noise (without signal) through a linear envelope detector results in a non-negative random voltage possessing Rayleigh statistics described by

$$p_1(v) = \frac{v\varepsilon}{\sigma^2}^{-\frac{v^2}{2\sigma}} \qquad 0 \le v < \infty \qquad (21)$$

where σ is the value of the noise prior to detection. (The noise will have a different RMS value after detection.)

On the other hand, the presence of a sinusoidal pulse (representing the return signal) results in a detected signal whose statistics are modified in a rather complex fashion. Let E represent the peak value of the sinusoidal pulse. It can now be shown that the probability density function of the detected signal plus noise can be described by the modified Rayleigh function

$$p_2(v) = \frac{v}{\sigma^2}\varepsilon^{-\frac{(v^2+E^2)}{2\sigma^2}} I_0\left(\frac{vE}{\sigma^2}\right) \qquad 0 \le v < \infty \qquad (22)$$

where $I_0(\ )$ is the modified Bessel function of the first kind, of order zero. The properties of this function are given in such mathematics references as Jahnke and Emde {3} and Hildebrand {4}.

For $E=0$, $p_2(v)$ of (22) reduces to $p_1(v)$ of (21) as should be expected since this case corresponds to noise only. On the other hand, it can be shown that as the argument of the I_0 function becomes large (order of magnitude of ten or greater), the asymptotic behavior of the Bessel function is such that the modified Rayleigh density function can then be approximated by the shifted Gaussian density function

$$p_2(v) \approx \frac{1}{\sqrt{2\pi}\sigma} \epsilon^{-\frac{(v-E)^2}{2\sigma^2}} \qquad \text{for } v>>1 \qquad (23)$$

This last expression is useful in calculations involving large signal-to-noise ratios.

For the modified Rayleigh statistics, the signal-to-noise ratio will be defined as the ratio of the RMS sinusoidal signal voltage to the RMS noise voltage.

$$s = \frac{E/\sqrt{2}}{\sigma} \qquad (24)$$

In decibels, this quantity can be expressed as

$$s(dB) = 10 \log_{10} \frac{E^2}{2\sigma^2} \qquad (25)$$

This definition actually corresponds to the conventional radar definition involving "peak power" (which is really the average sinusoidal power during the duration of the pulse).

As in the Gaussian case, it is convenient to normalize the voltage and threshold scales with the forms

$$x = \frac{v}{\sigma} \tag{26}$$

$$a = \frac{A}{E} \tag{27}$$

A closed form expression may be determined for p. It is given by

$$p = \int_0^A p_1(v)dv \tag{28}$$

Solution of this integral yield

$$p = 1 - \varepsilon^{-(as)^2} \tag{29}$$

Development of an expression for q with use of the various preceding definitions yields

$$q = \int_{as}^{\infty} x\varepsilon^{-\frac{x^2}{2}} \varepsilon^{-s^2} I_0(\sqrt{2}sx)dx \tag{30}$$

Actually, in many cases, it is more convenient to evaluate (30) by integrating from zero to as and arranging the desired result as follows:

$$q = 1 - \int_0^{as} x\varepsilon^{-\frac{x^2}{2}} \varepsilon^{-s^2} I_0(\sqrt{2}sx)dx \tag{31}$$

V. EVALUATION TECHNIQUES

Numerical integration techniques were employed in the evaluation of all the preceding integrals except for the p parameter in the Rayleigh case, which was readily evaluated in closed form as expressed by (29). The various parameters such as altitude and signal-to-noise ratio were varied over a wide range of values corresponding to realistic operating requirements of the intended application. The range of parameter values and the results of the evaluations will be discussed in the next section. An IBM 1130 digital computer was employed for the computations using FORTRAN IV with scientific subroutines.

The closed-form expression for $\bar{n}$ given by (8) was used in obtaining data at low signal-to-noise ratio. However, for high signal-to-noise ratios, the value of p approaches unity so closely that a nearly indeterminate form was encountered in this evaluation, and considerable computer error resulted. This problem was solved by returning to the basic definition of $\bar{n}$ as expressed by (7) for the calculations at the higher signal-to-noise ratios. Some overlap in the data obtained from the separate approaches was utilized to determine the appropriate range in which the closed-form approach was accurate.

Some difficulty was encountered in the solution of the integrals involving the probability density

functions. As previously observed, the probability density function for the modified Rayleigh case contained a zero-order modified Bessel function of the first kind. Although the scientific subroutine package available with the IBM 1130 contained a solution for this function, the range of the argument was limited to 60. Since this range was insufficient, it was necessary to utilize the fact that for large arguments, the modified Rayleigh function can be approximated by a Gaussian function as given by (23). Therefore, for small arguments of the Bessel function, the available subroutine was employed in the evaluation, but for arguments greater than 60, the Gaussian approximation was substituted.

The integration of the Gaussian density function itself precipitated another problem. As the upper limit of the integral of the Gaussian density function increased to the point that the accumulative probability approached unity, the rounding and truncation errors in the numerical integration technique became intolerable. This problem was solved by interfacing the numerical integration with an asymptotic series approximation for the Gaussian distribution in the region where errors became significant. The approximation for the Gaussian function was derived from the asymptotic series approximation for the error function.

VI. DISCUSSION OF GAUSSIAN DATA

The prototype Altitude Measuring Unit developed at Langley Research Center possesses the following design parameters:

(1) maximum desired altitude = 200,000 ft.

(2) pulse repetition rate = 1 kHz

(3) pulse width = 1 μs

(4) 3 dB bandwidth of low-pass filter (Butterworth characteristic) employed in simulation = 500 kHz

Observe that the total period of a cycle (1 ms) is approximately 2.5 times the total delay corresponding to an altitude of 200,000 ft. The additional time interval was chosen to minimize the possible ambiguity resulting from so-called "second-time-around" targets. On the other hand, the additional time interval results in a higher percentage of late false alarms, and the effect of varying this time interval will be discussed later.

Using the data above, the total number of assumed independent samples in a period is readily calculated by (2) to be

j = 1000 samples

The value of i will be directly proportional to the altitude. As a matter of computational convenience, the value of i was rounded off to be 2 samples per thousand feet of altitude. Since there is some uncertainty

regarding the exact number of statistically independent samples anyway, it is felt that this assumption introduces negligible error. The values of altitude employed in the study and the corresponding values of i are given below:

Altitude	i
12,500 ft.	25
25,000 ft.	50
50,000 ft.	100
100,000 ft.	200
200,000 ft.	400

At each altitude the signal-to-noise ratio was varied from 1 dB to 30 dB in steps of 1 dB. The computations were first performed with Gaussian statistics.

The first phase of the data to be presented is a comparison between some experimental data taken at LRC and the corresponding computer data as a means of verifying the accuracy of the computer model. Using the 2BT formulation for the computer run, the comparison is shown in Fig. 6. (Recall that a is the ratio of threshold level to peak signal level as defined in Section III.) Considering all of the assumptions that have been made, the agreement of the different sets of data is quite impressive. From this point on, the computer data will be used exclusively, since only a limited amount of experimental data is available.

Before presenting any further extensive data, a brief pause will be made at this point to show the sensitivity of the data to changing the number of independent samples from 2BT to BT. This momentary change required a change in format from 1000 total samples to 500 samples, and it reduced the parameter i to 1 sample per thousand feet. In order to compare this data both with experimental data and with 2BT data, the parameters for this run were chosen the same as were employed for Fig. 6. A comparison between the data obtained for the BT computer calculations and the 2BT computer calculations is shown in Fig. 7. Note that the 2BT data is merely a repeat of the data given in Fig. 6.

Comparison of the two sets of curves in Fig. 7 and reference back to Fig. 6 results in the following conclusions:

(1) The data obtained from the computer calculations are not especially sensitive to changes in the number of independent samples assumed, at least not over the range from 2BT to BT. The sets of curves are almost identical in form and are displaced from each other horizontally, at most, by about 1 dB.

(2) The data obtained from the 2BT assumption are much closer in agreement with the experimental data than the data obtained from the BT assumption.

On the basis of these conclusions, the remainder of the data to be presented was obtained from the 2BT assumption outlined at the beginning of this section.

A compilation of the expected results with Gaussian statistics is provided in Figures 8 through 12 on each figure, curves of the relative altimeter reading versus the SNR with the relative threshold level as a parameter are presented. Each figure corresponds to a fixed altitude.

As a matter of understanding (and academic interest perhaps), a different form of presentation of the preceding data is given in Figures 13 through 17. On each figure, curves of the relative altimater reading versus the altitude for a fixed SNR and with the relative threshold level as a parameter are presented. The impracticality of these curves lies in the assumption that the SNR would be constant as the altitude varies. Nevertheless, these results provide some interesting information regarding the behavior of the data.

The data presented so far were developed from Gaussian statistics, which were employed in all of the experimental data. No attempt has been made yet to discuss optimum threshold settings and required signal-to-noise ratios for the intended application, since the actual space system will involve a detected bandpass signal whose statistics are Rayleigh in nature. A consideration of this case will be made in the next section.

VII. DISCUSSION OF RAYLEIGH DATA

The data to be discussed in this section were obtained from computer calculations employing Rayleigh and modified Rayleigh statistics as discussed in Section IV. The four assumptions stated at the beginning of Section VI were employed throughout (except for a few later runs in which the pulse repetition rate was varied). No experimental data was available in this case, but in view of the excellent correlation of the Gaussian data, a high degree of confidence is held in the results obtained.

A compilation of the expected results employing Rayleigh statistics is provided in Figures 18 through 22. The desired type of behavior would be a curve approaching unity level for as small a SNR as possible, with no further overshoot as the SNR increases. At the lower altitudes a threshold setting of approximately 0.5 E would appear to be about optimum. On the other hand, at an altitude of 200,000 ft., a threshold setting closer to 0.6 E appears to be more optimum. Since the SNR of a practical altimeter would ordinarily increase as the altitude decreases, the highest altitude would be the case of most critical concern.

The basic radar equation {1}, {2} predicts that, if all other factors are unchanged, the signal-to-noise ratio of a given bistatic radar receiver will increase by

12 dB if the altitude is halved. Inspection of Figures 21 and 22 reveals that if the threshold level is set at 0.6 E at 200,000 ft., the additional gain in signal-to-noise ratio as the altitude is reduced far more than compensates for the slight deviation from the non-ideal threshold setting at lower altitudes.

In line with the preceding paragraph, it can be seen that from over the range from about 0.4 E to about 0.6 E, there is not an excessive degree of change in the behavior of the curves. On the other hand, if the threshold level becomes too small, a very high signal-to-noise ratio is required to achieve accuracy. Finally, if the threshold level is set too high, very erratic behavior and high readings are observed, especially at low altitudes. These phenomena indicate that the behavior of the Automatic Gain Control (AGC) must be carefully constrained to either maintain a constant signal level at all altitudes, or at least to ensure that the effect of variation in threshold due to non-ideal AGC is more than offset by the increased signal-to-noise ratio as the altitude is decreased.

As a final topic of interest, the pulse repetition frequency was increased to 2 kHz, and curves were generated at altitudes of 100,000 ft. and 200,000 ft. Observe that this changes the total number of independent samples in a period from 1000 to 500, while maintaining

the 2BT constraint. The results are shown in Figures 23 and 24. Comparing these curves with the corresponding curves of Figures 21 and 22, the "overshoot" phenomena is seen to be reduced at the higher prf as a result of fewer late false alarms, but the behavior in the vicinity of the optimum threshold setting is not drastically affected. Thus, it appears that the pulse repetition rate originally chosen is probably quite acceptable if adequate AGC is maintained.

VIII. CONCLUDING REMARKS

A mathematical model capable of predicting the reading of an AM-CW radar altimeter has been developed. The model has been successfully implemented in a comprehensive digital computer program on an IBM 1130. The input data to the program includes (1) statistics of the noise and signal plus noise, (2) altitude, (3) signal-to-noise ratio, and (4) threshold level setting.

Comprehensive data were taken from computer runs assuming Gaussian statistics in order to provide correlation with certain data available from Langley Research Center and to establish the general behavior of a system in which these statistics are valid. The computer data were found to be in very close agreement with the available measured data.

Inasmuch as the study was related to a proposed planetary altimeter design, extensive data were taken with assumed Rayleigh and modified Rayleigh statistics, which represents the appropriate statistics at the output of a linear envelope detector.

From the data obtained corresponding to an altitude of 200,000 ft., a minimum pre-detector signal-to-noise ratio of about 15 dB appears to be absolutely necessary for good accuracy. The corresponding threshold setting is about 60% of the peak signal amplitude.

REFERENCES

{1} Skolnik, Merrill I., Introduction to Radar Systems. McGraw-Hill Book Co., New York, 1962.

{2} Barton, David K., Radar System Analysis. Prentice-Hall, Inc., Englewood Cliffs, 1964.

{3} Jahnke, E., and Emde F., Tables of Functions. 4th ed., Dover, New York, 1945.

{4} Hildebrand, F. B., Advanced Calculus for Engineers. Prentice-Hall, Inc., Englewood Cliffs, 1949.

APPENDIX

SUMMATION FORMULAE

$$\sum_{i}^{j} p^n = \frac{p^i - p^{j+1}}{1-p} \qquad \text{(A1)}$$

$$\sum_{i}^{j} np^n = \frac{ip^i - jp^{j+1}}{1-p} + \frac{p^{i+1} - p^{j+1}}{(1-p)^2} \qquad \text{(A2)}$$

$$\sum_{i}^{j} n^2 p^n = \frac{i^2 p^i - j(j+1)p^{j+1}}{1-p}$$

$$+ \frac{(2i+1)p^{i+i} - (j+1)p^{j+1} - jp^{j+2}}{(1-p)^2} \qquad \text{(A3)}$$

$$+ \frac{2(p^{i+2} - p^{j+2})}{(1-p)^3}$$

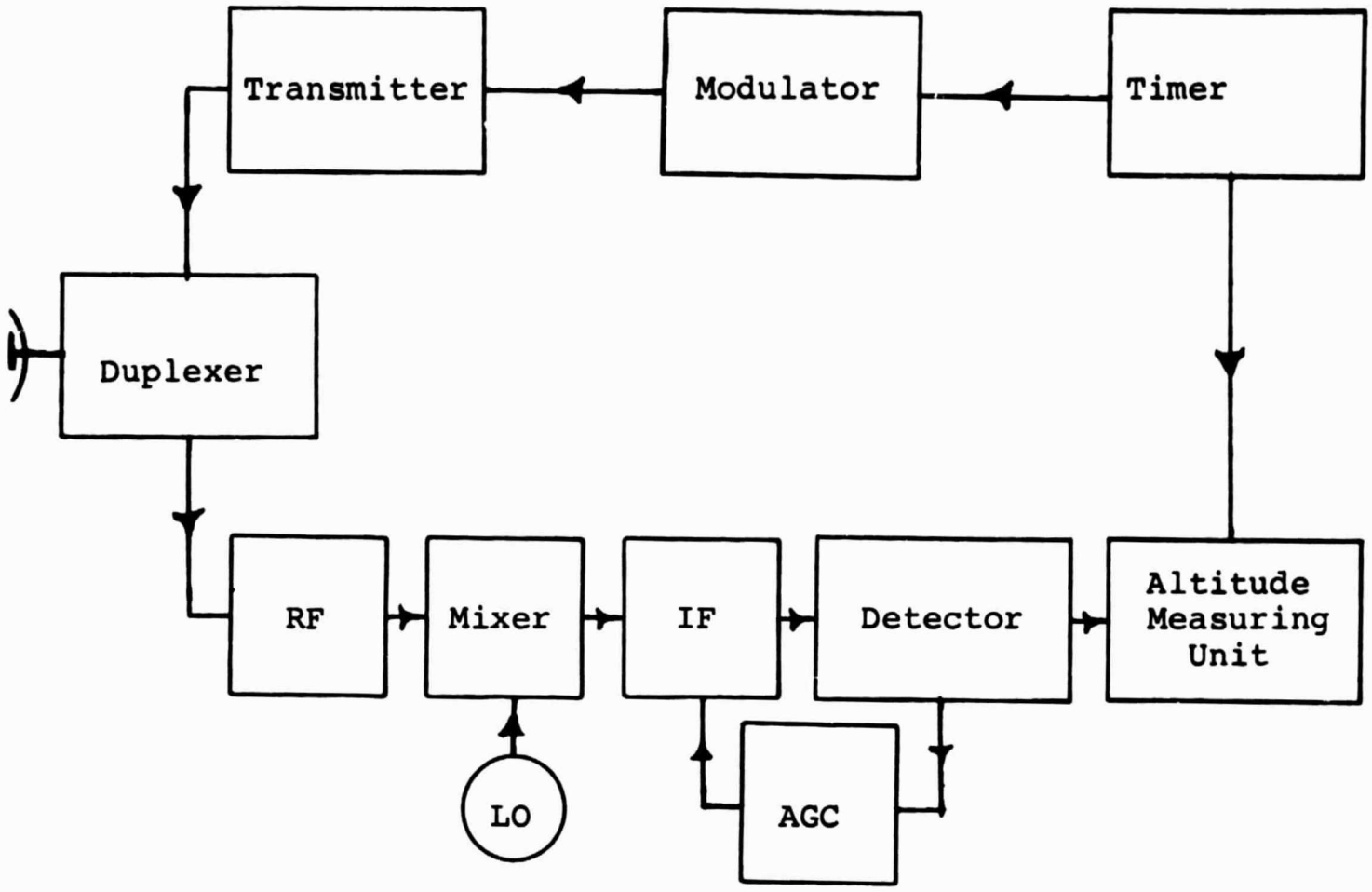

Fig. 1. Block diagram of radar.

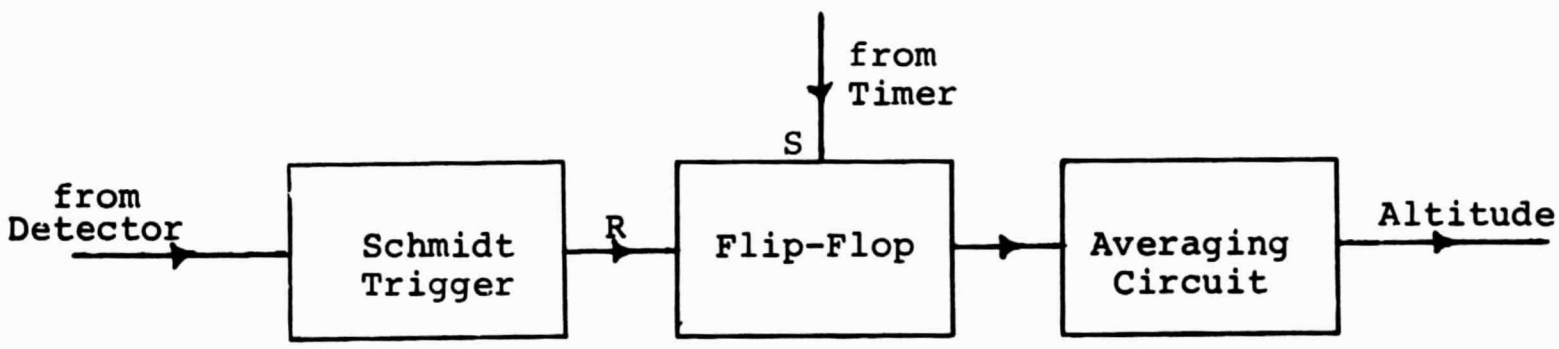

Fig. 2. Block diagram of altitude measuring unit.

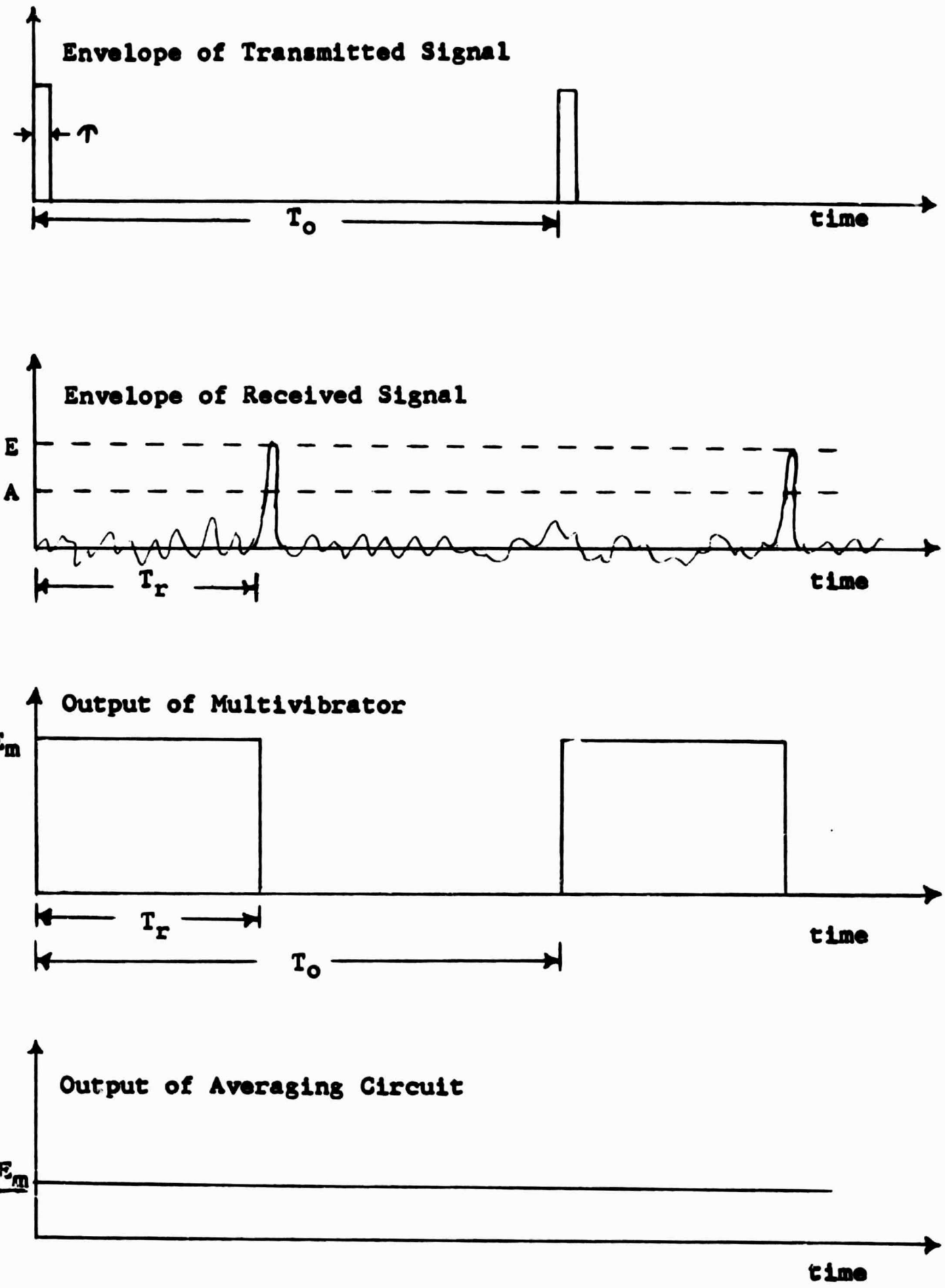

Fig. 3. Waveforms in radar system.

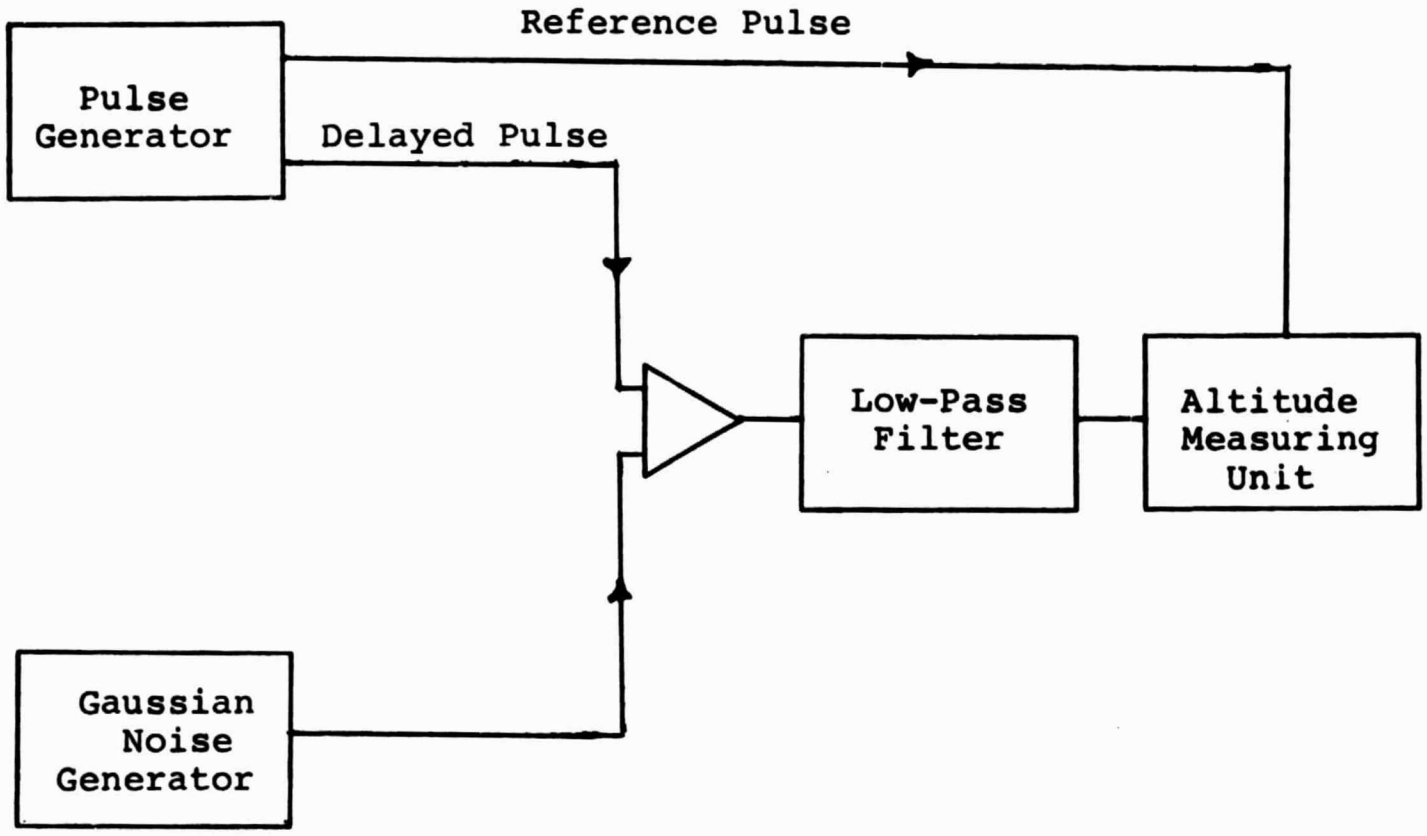

Fig. 4. Block diagram of prototype simulation system.

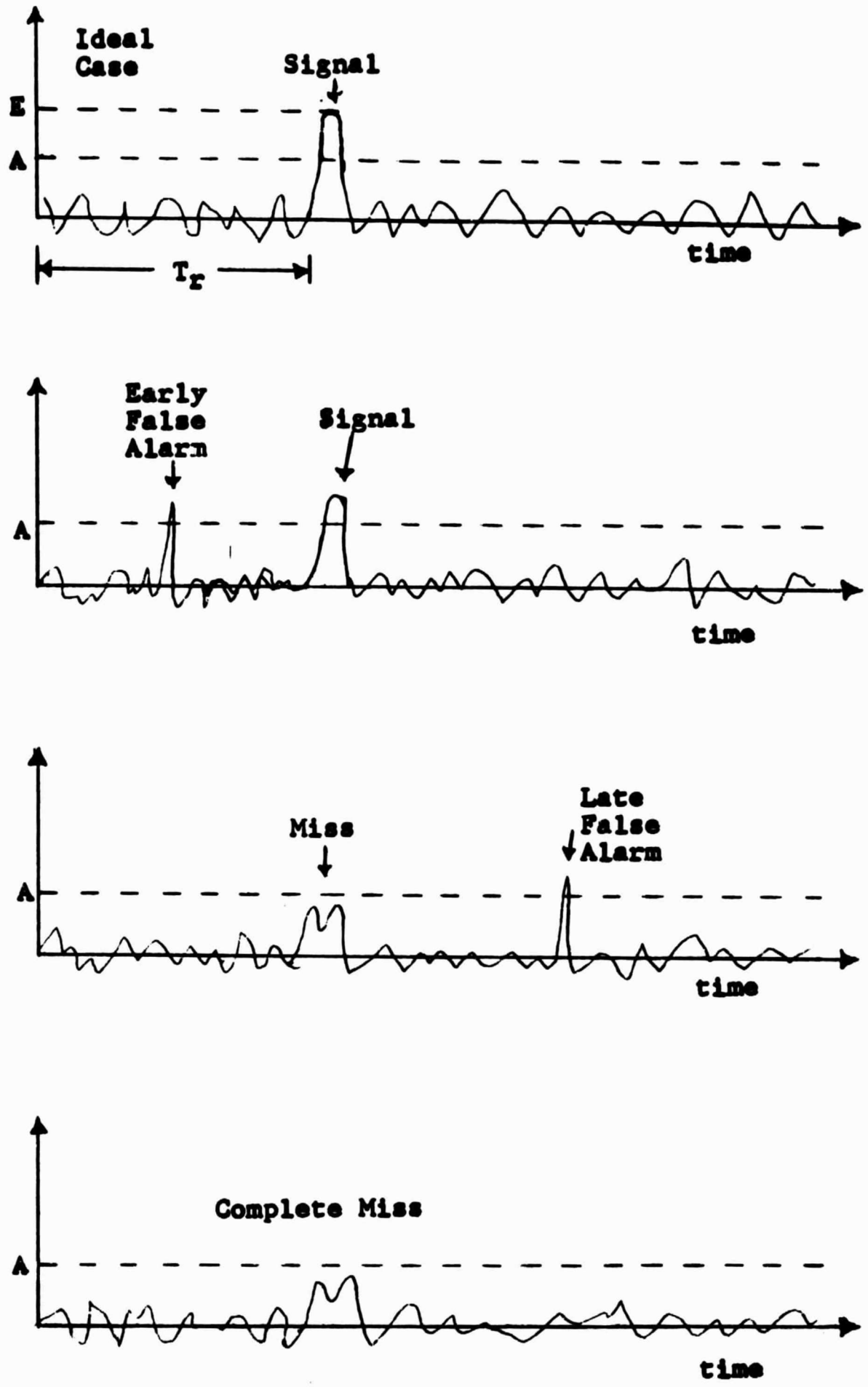

Fig. 5. Possible trigger outcomes in AMU.

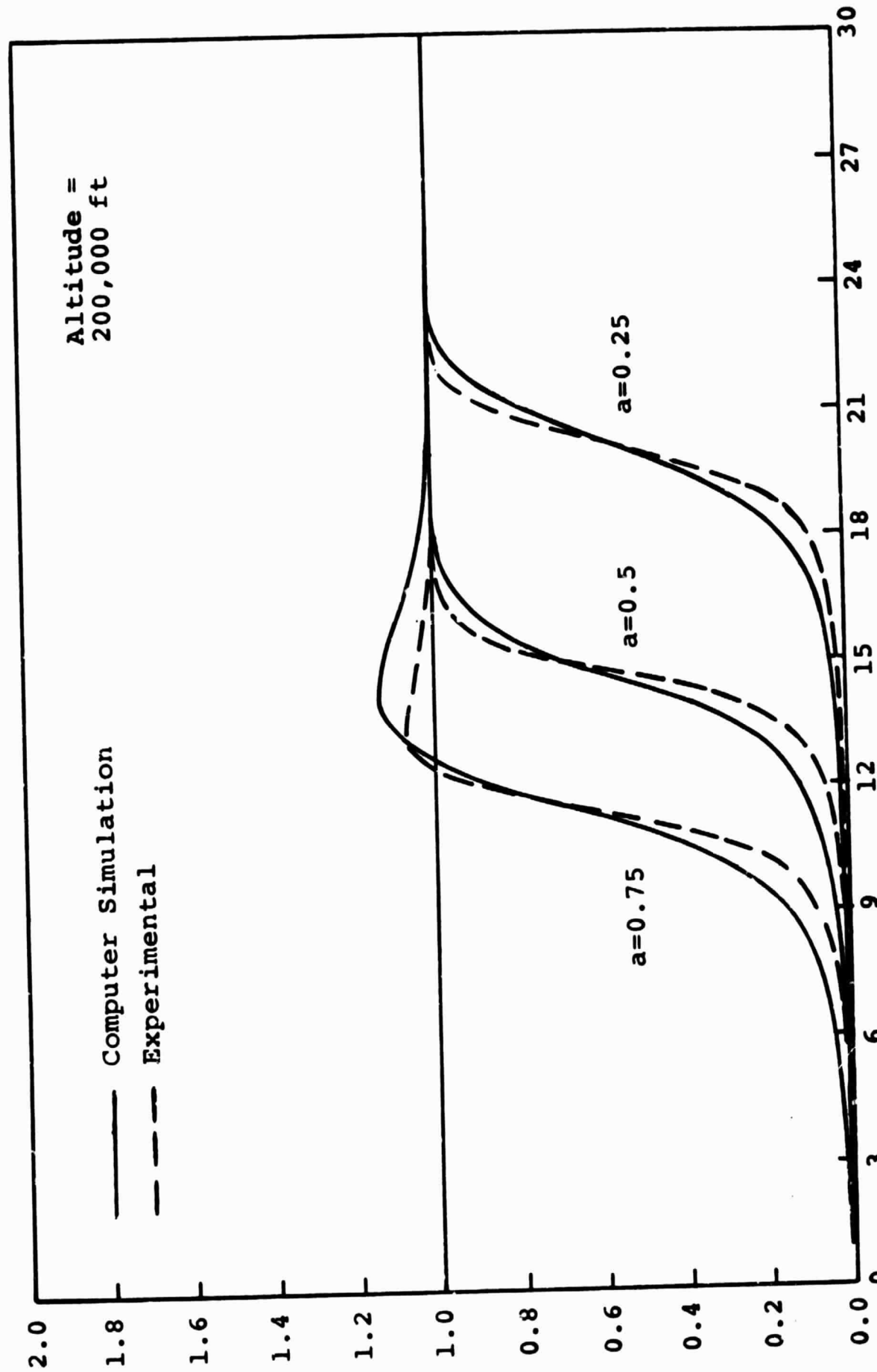

Fig. 6. Comparison of certain experimental data and computer simulation results with Gaussian statistics.

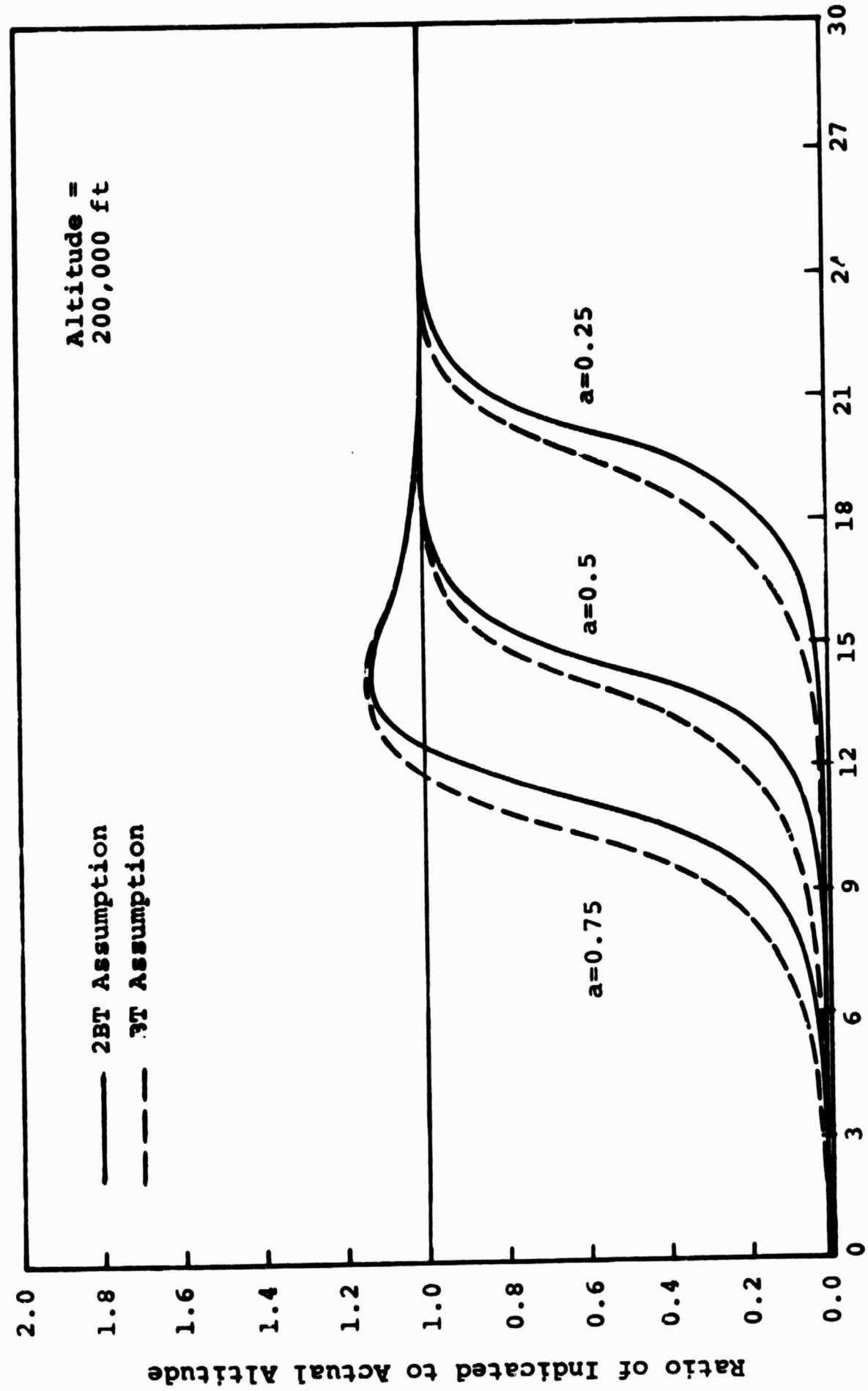

Fig. 7. Effects of changing the assumed number of independent samples with Gaussian statistics.

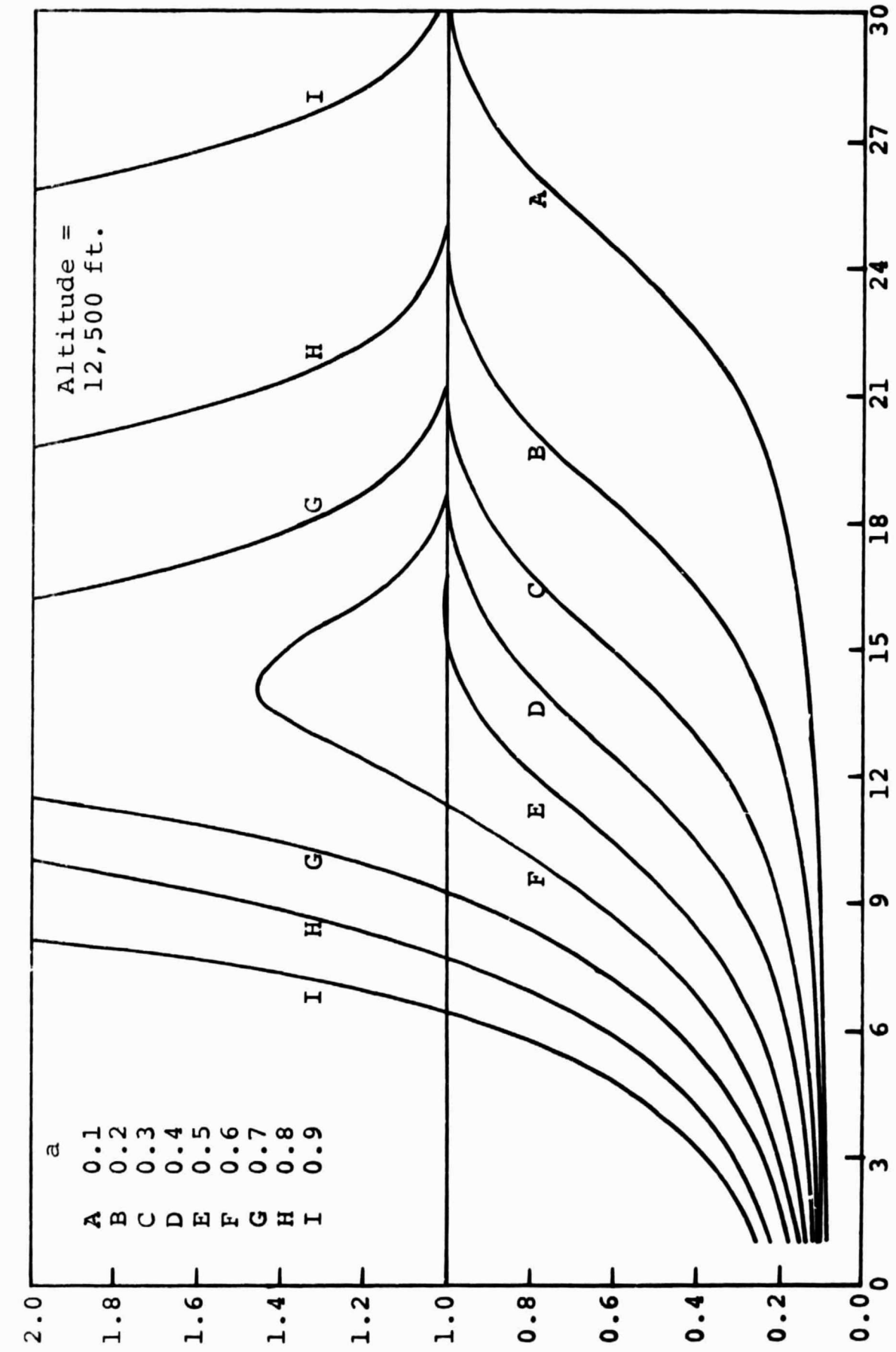

Fig. 8. Predicted performance with Gaussian statistics at 12,500 ft.

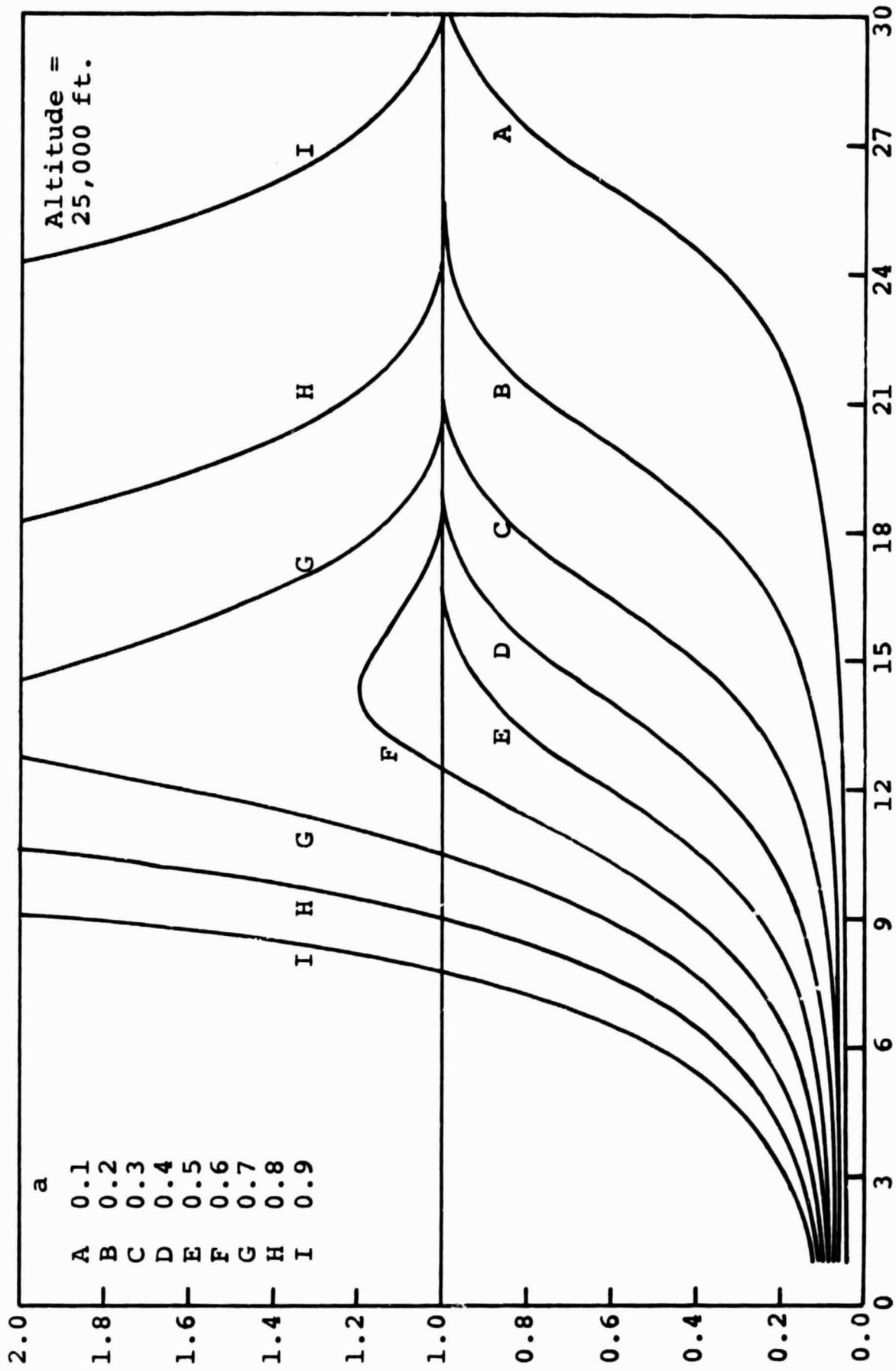

Fig. 9. Predicted performance with Gaussian statistics a

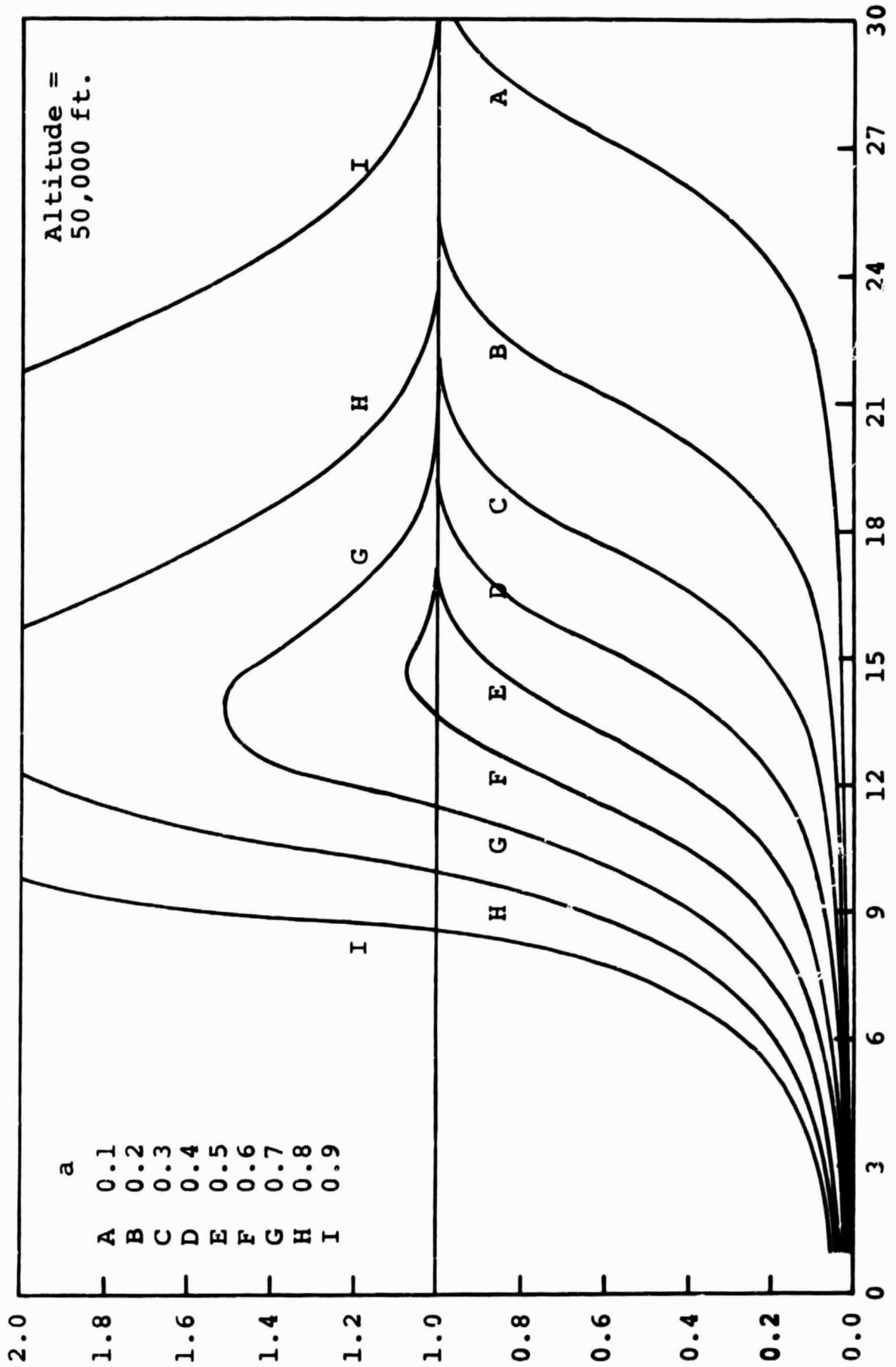

Fig. 10. Predicted performance with Gaussian statistics at 50,000 ft.

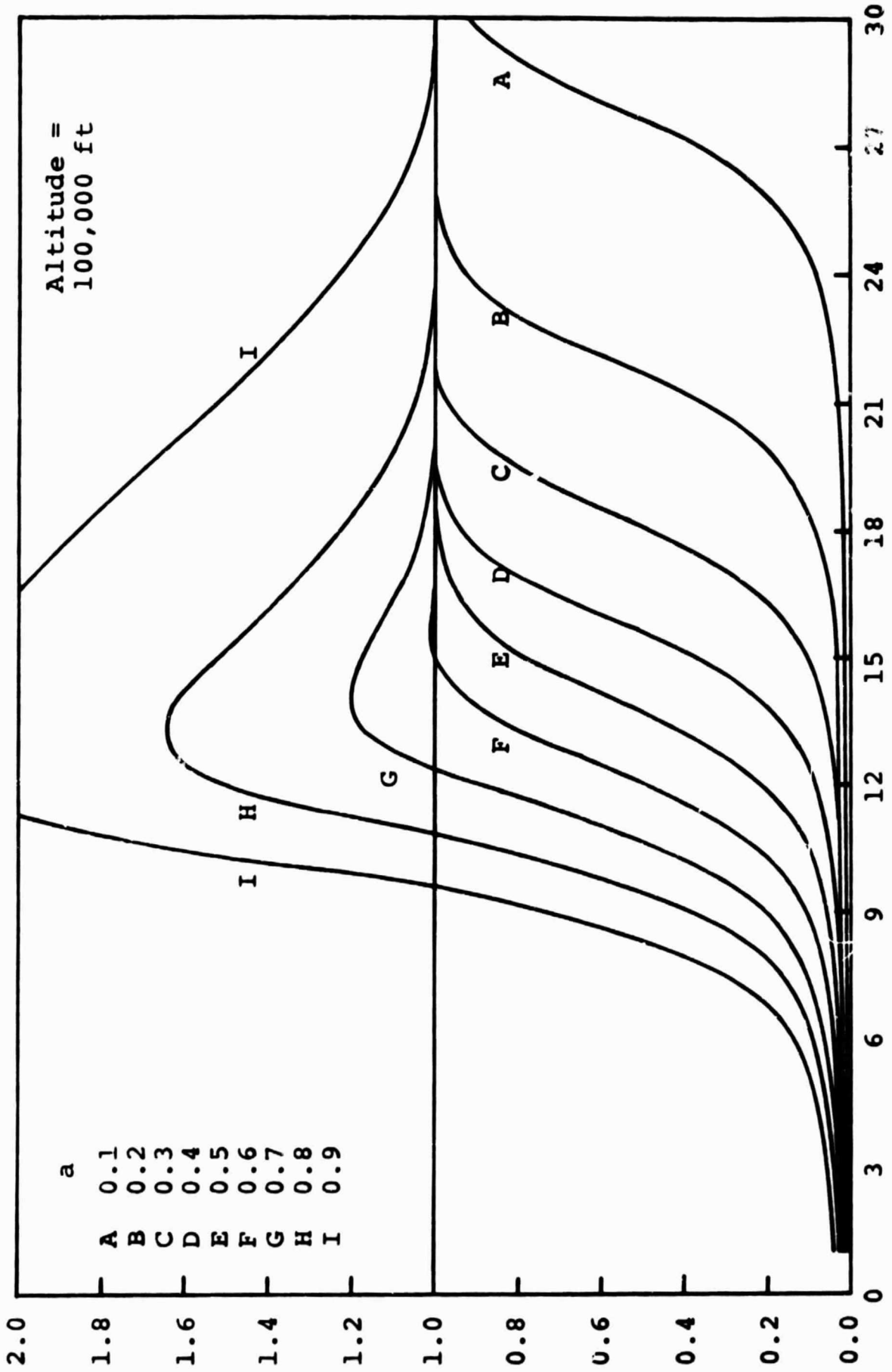

Fig. 11. Predicted performance with Gaussian statistics at 100,000 ft.

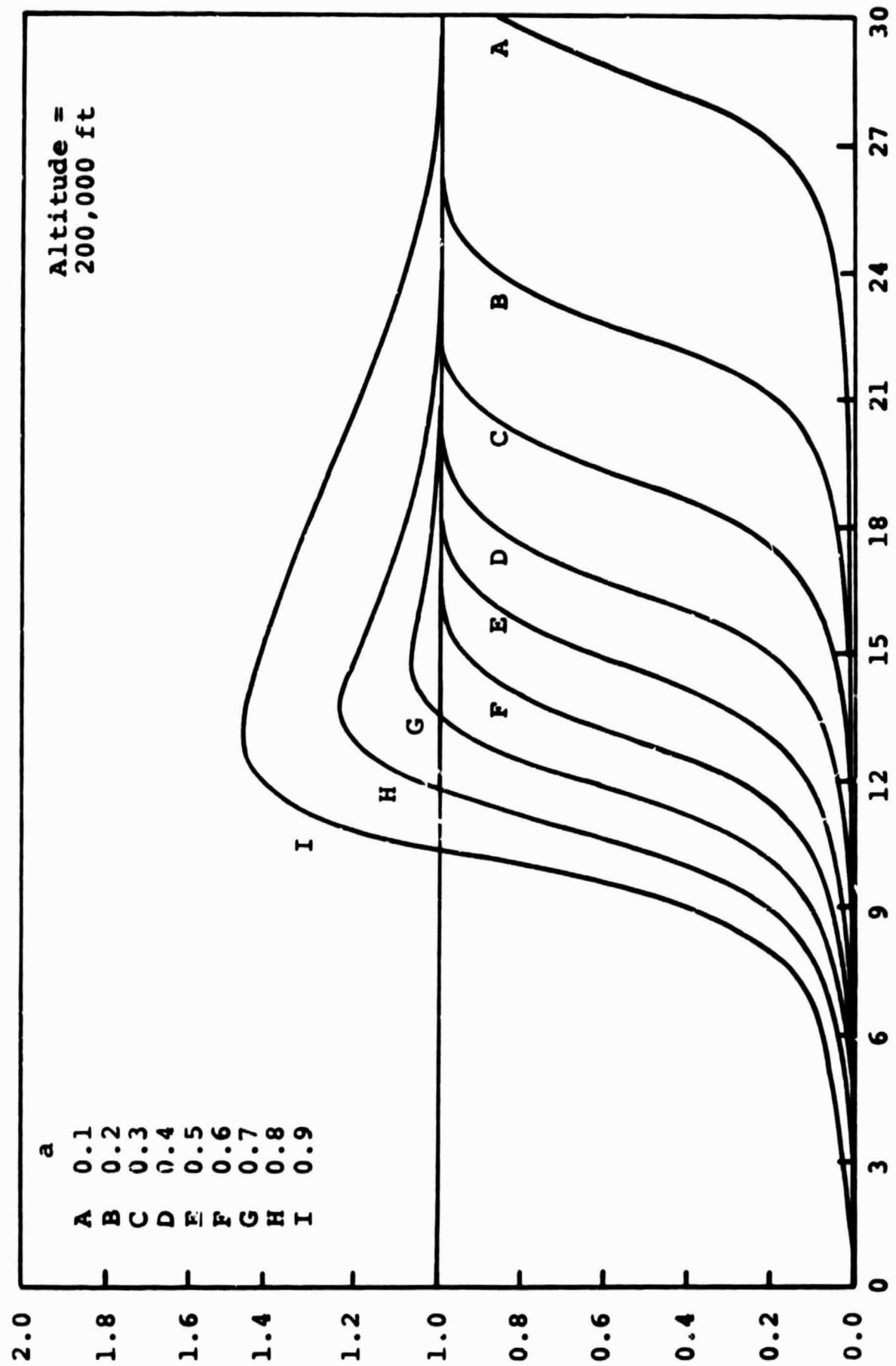

Fig. 12. Predicted performance with Gaussian statistics at 200,000 ft.

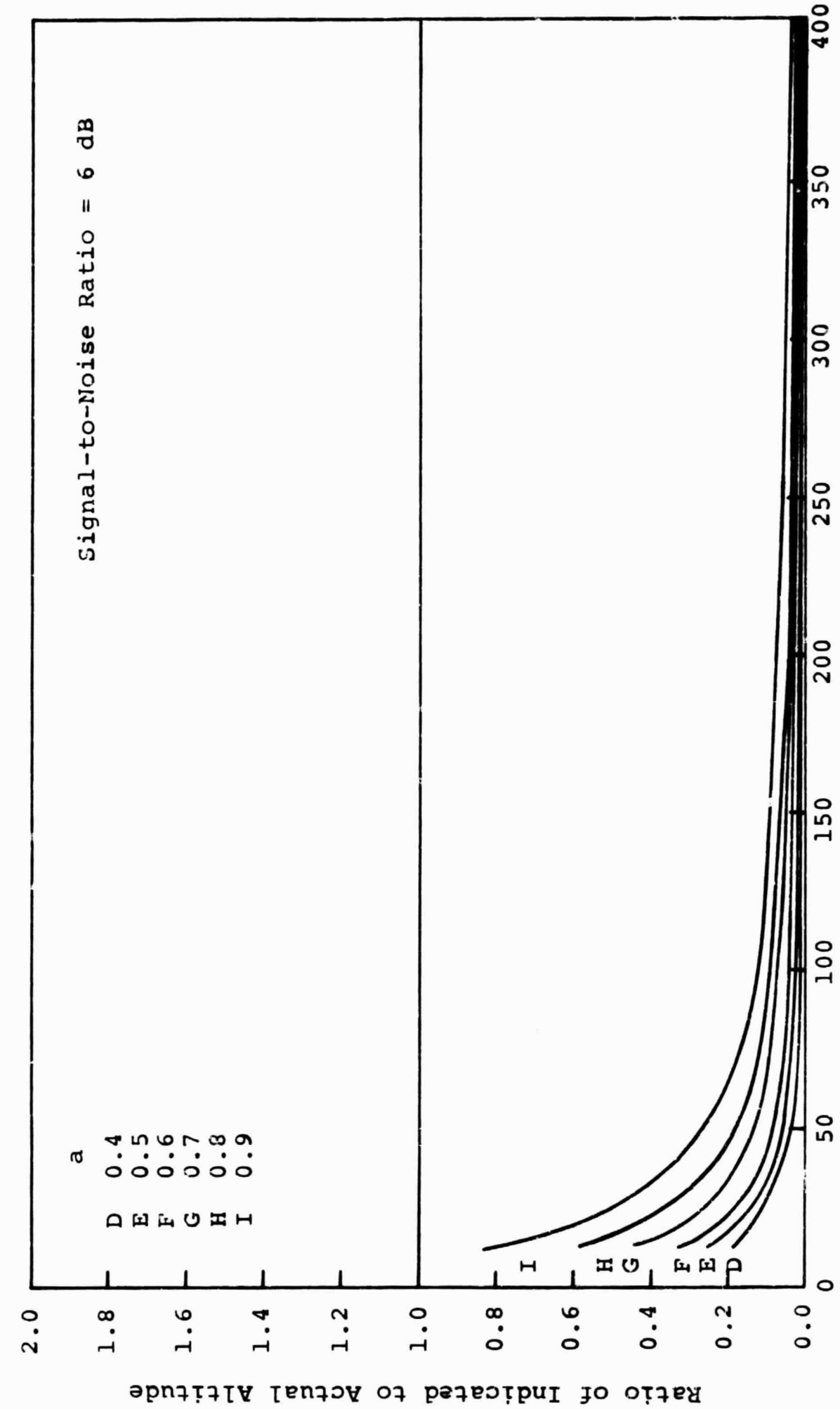

Fig. 13. Predicted performance with Gaussian statistics at SNR = 6 dB

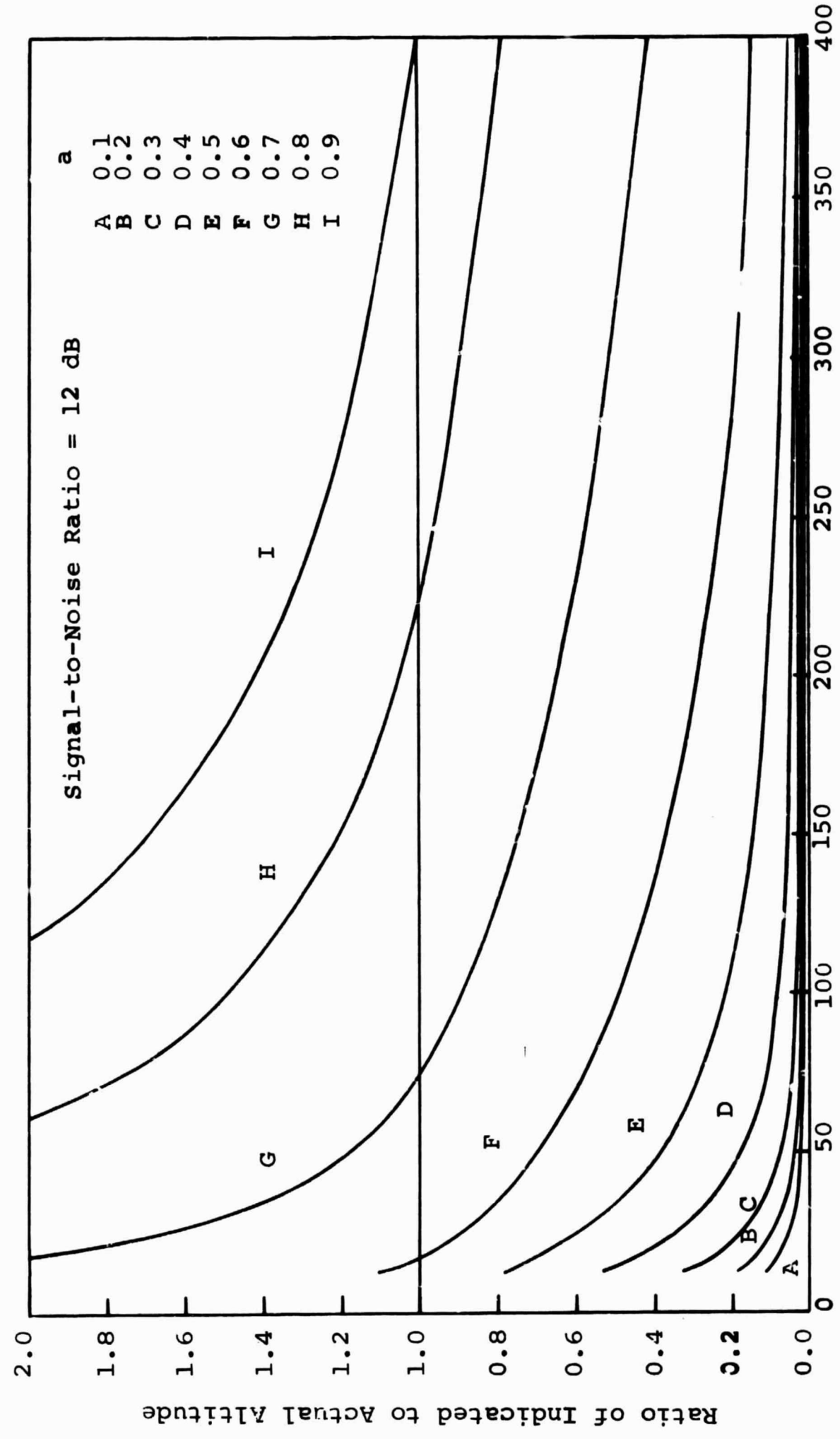

Fig. 14. Predicted performance with Gaussian statistics at SNR = 12 dB.

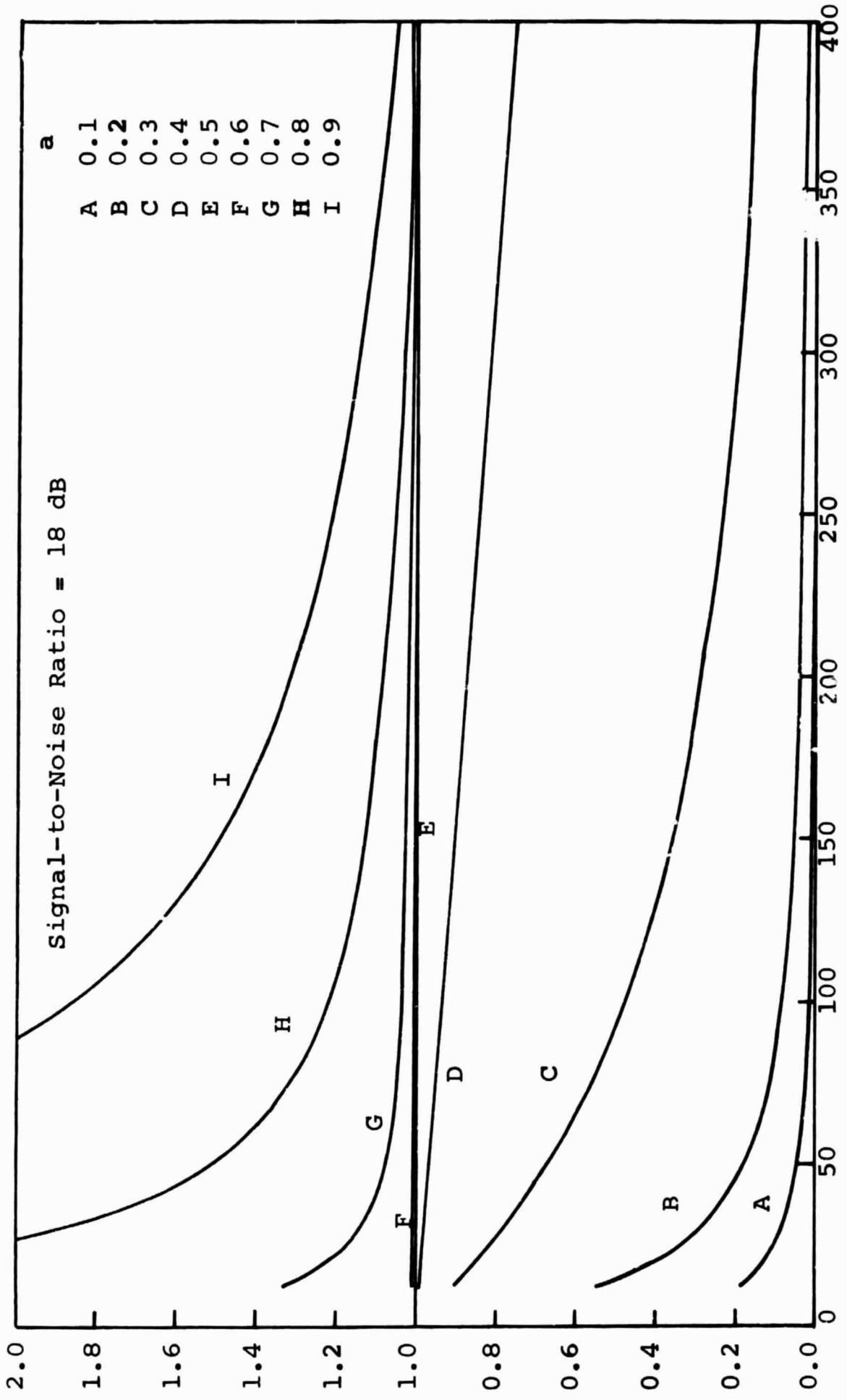

Fig. 15. Predicted performance with Gaussian statistics at SNR = 18 dB.

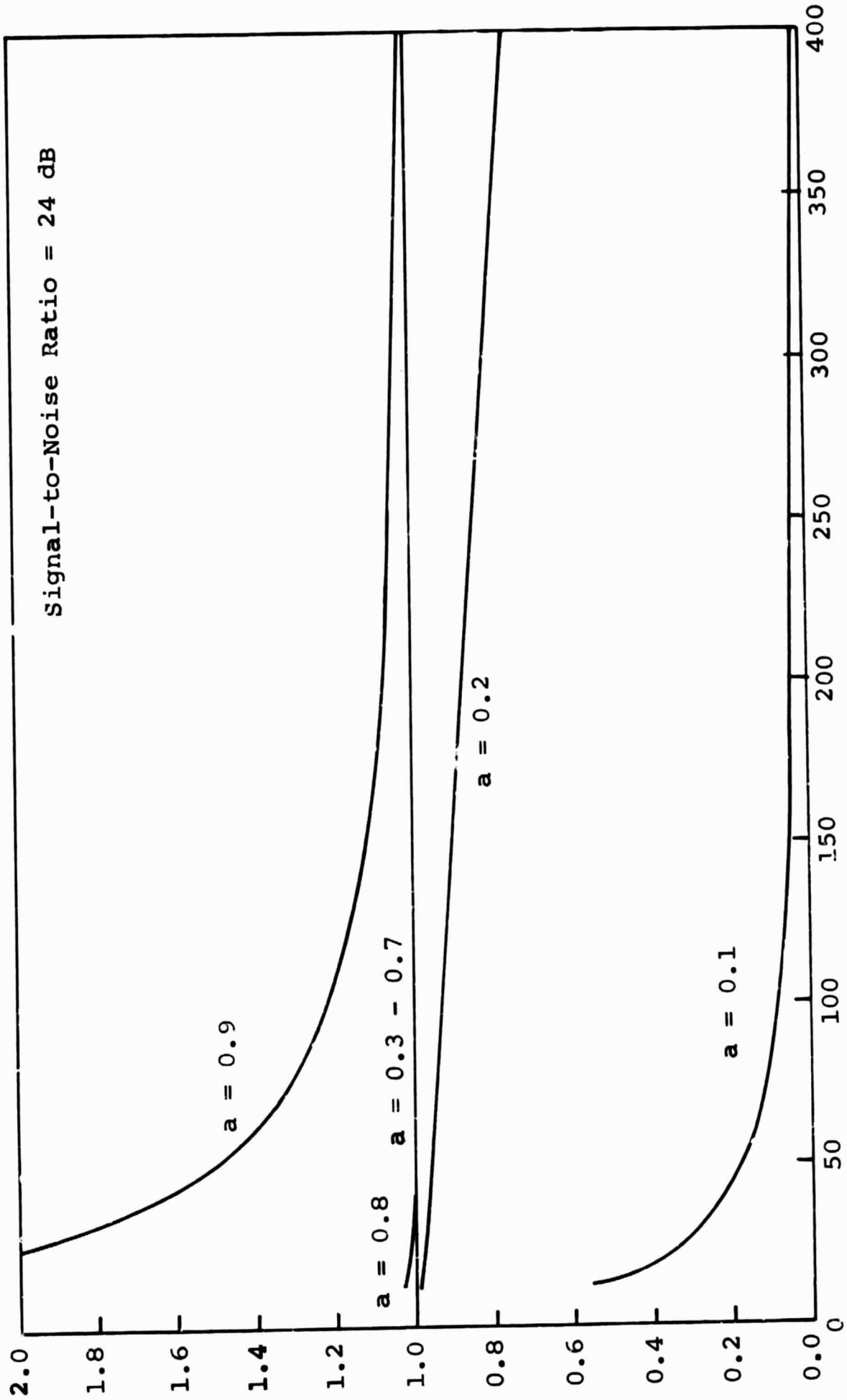

Fig. 16. Predicted performance with Gaussian statistics at SNR = 24 dB.

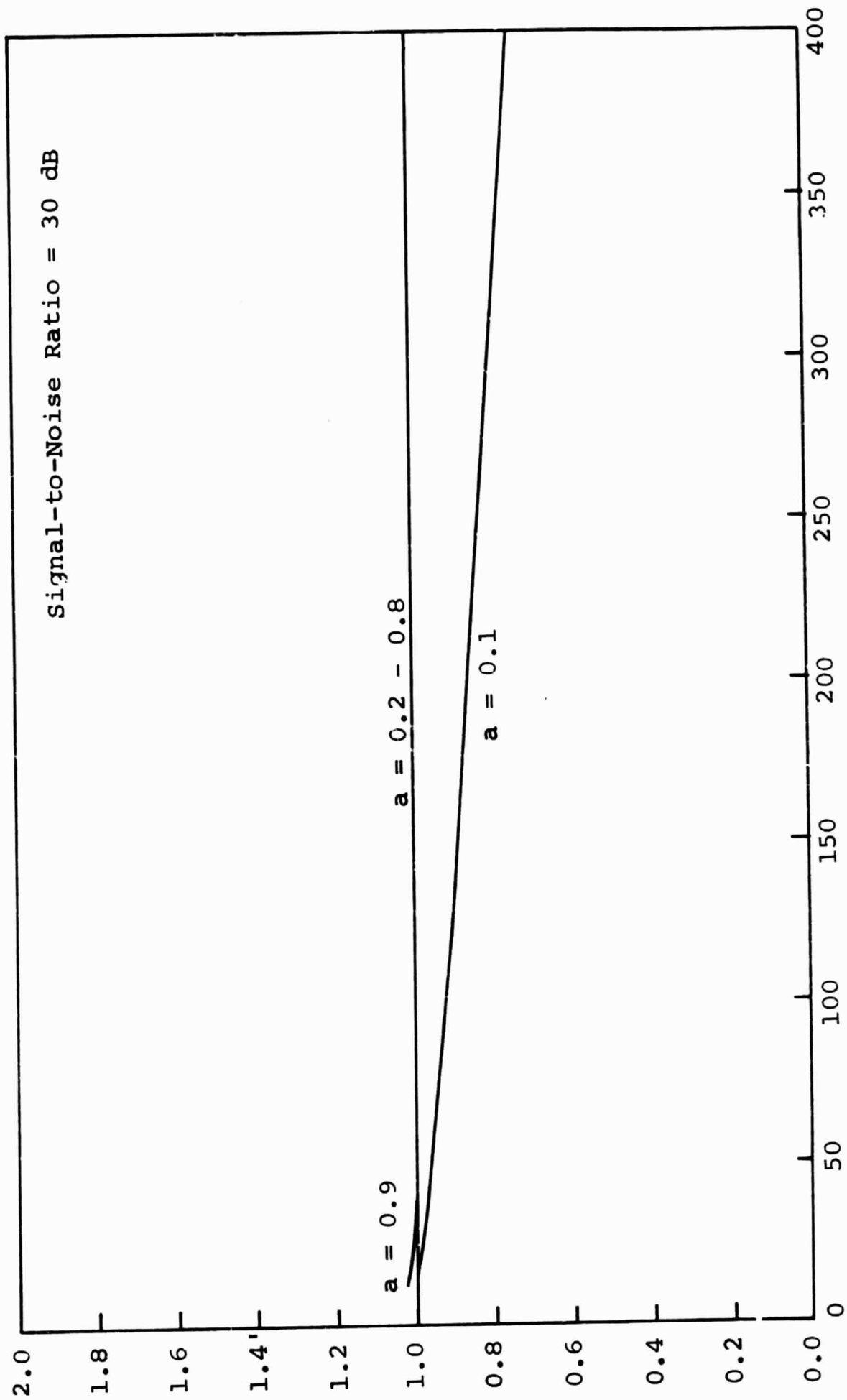

Fig. 17. Predicted performance with Gaussian statistics at SNR = 30 dB.

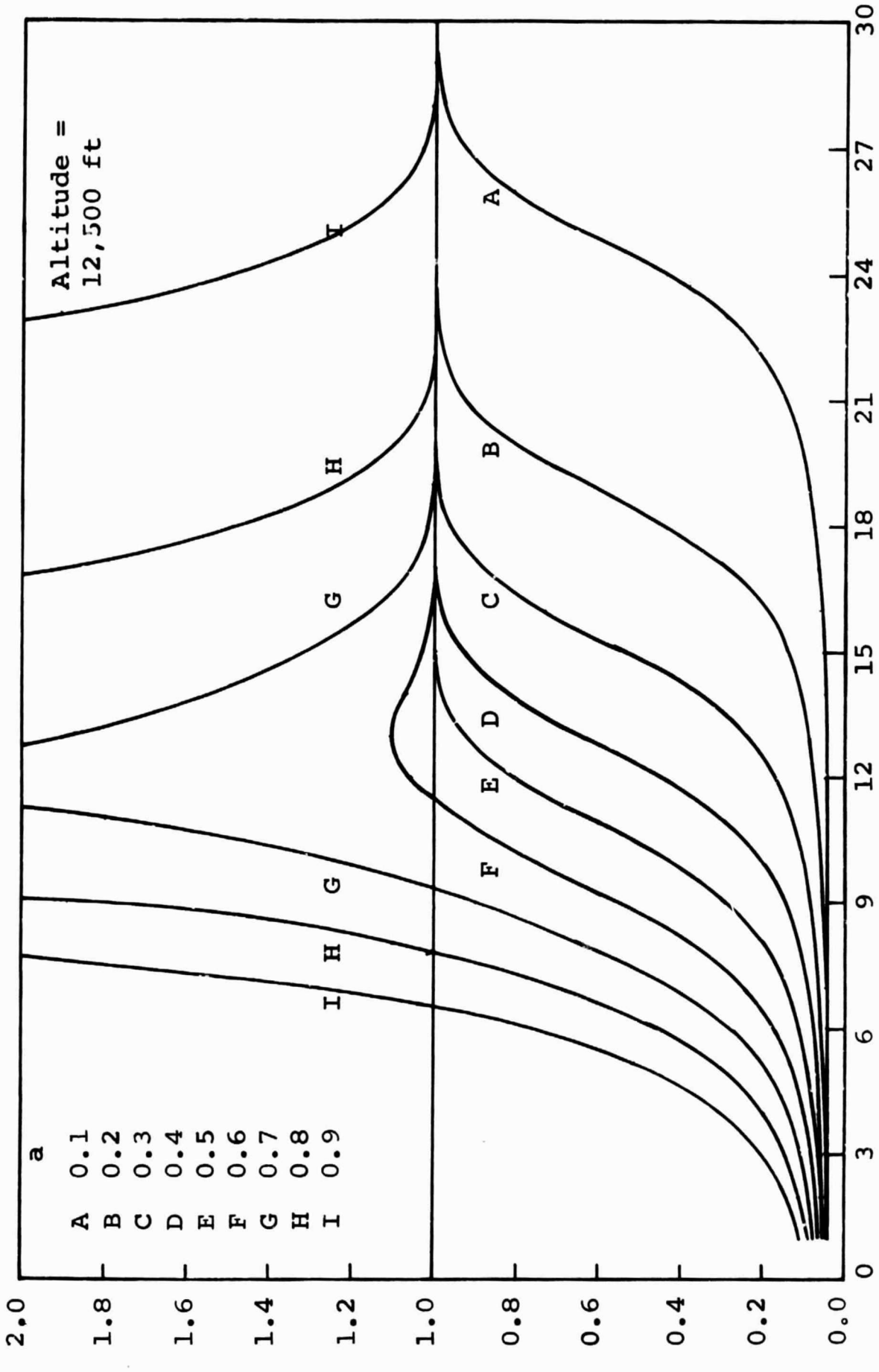

Fig. 18. Predicted performance with Rayleigh statistics at 12,500 ft.

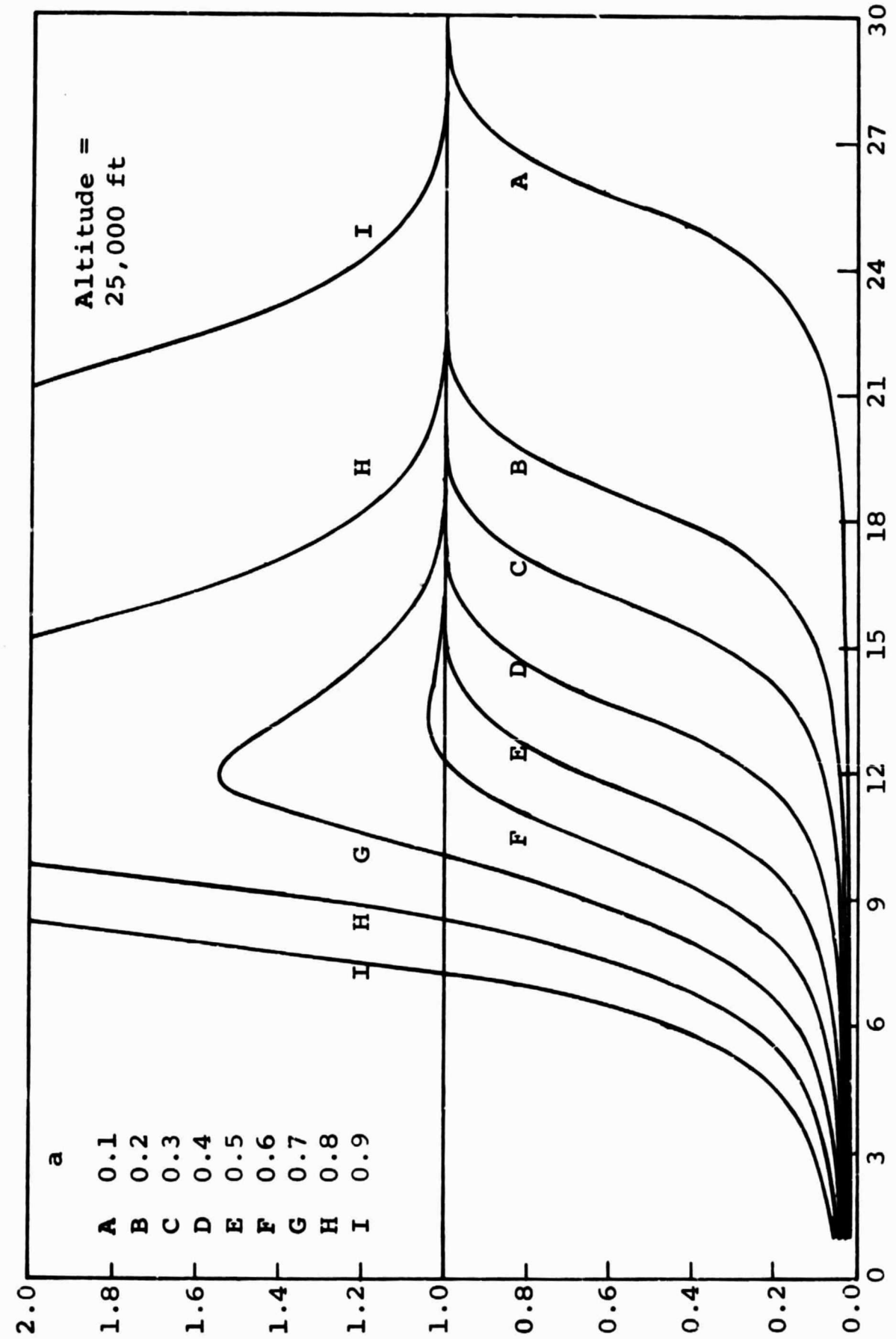

Fig. 19. Predicted performance with Rayleigh statistics at 25,000 ft.

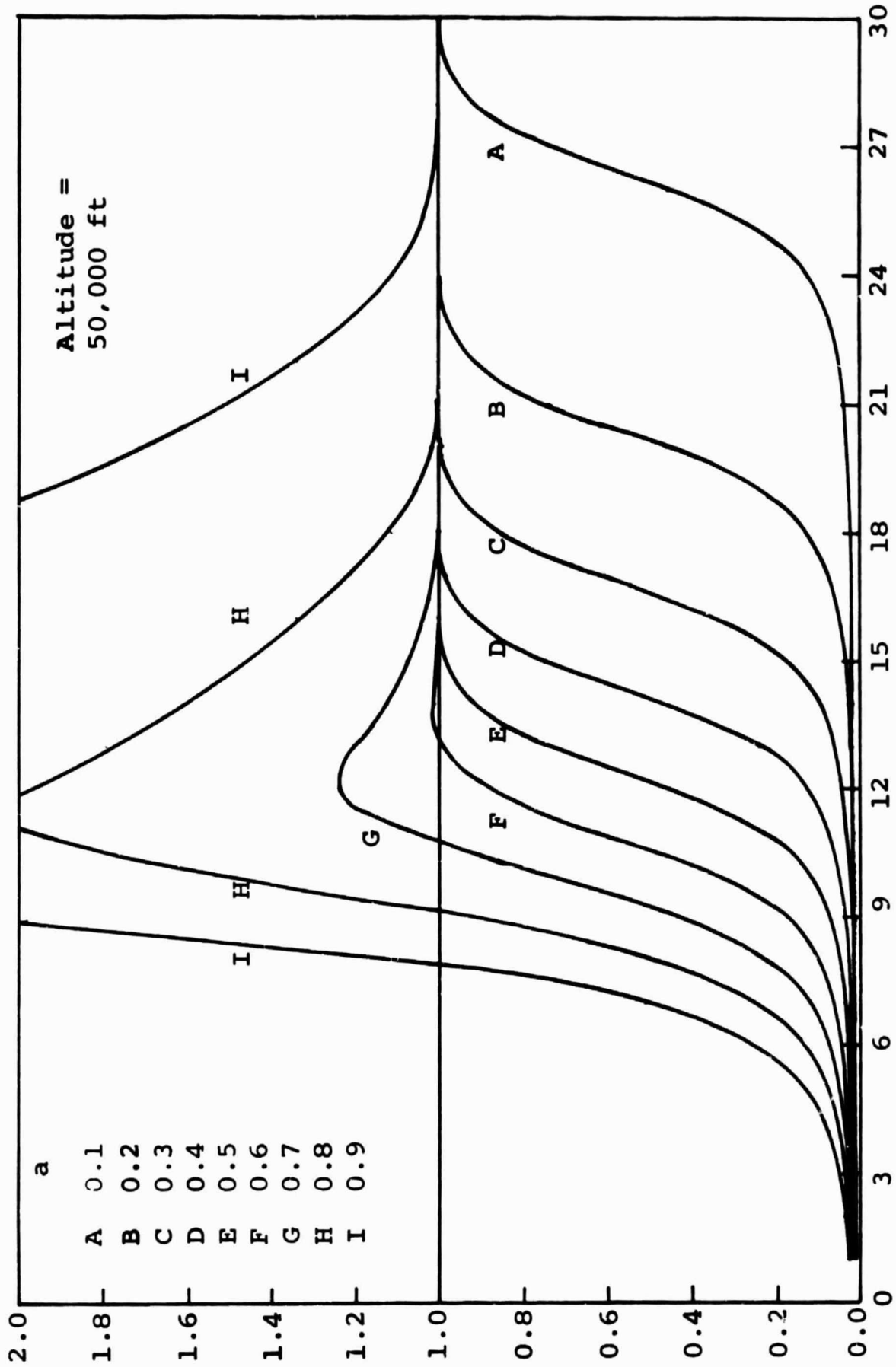

Fig. 20. Predicted performance with Rayleigh statistics at 50,000 ft.

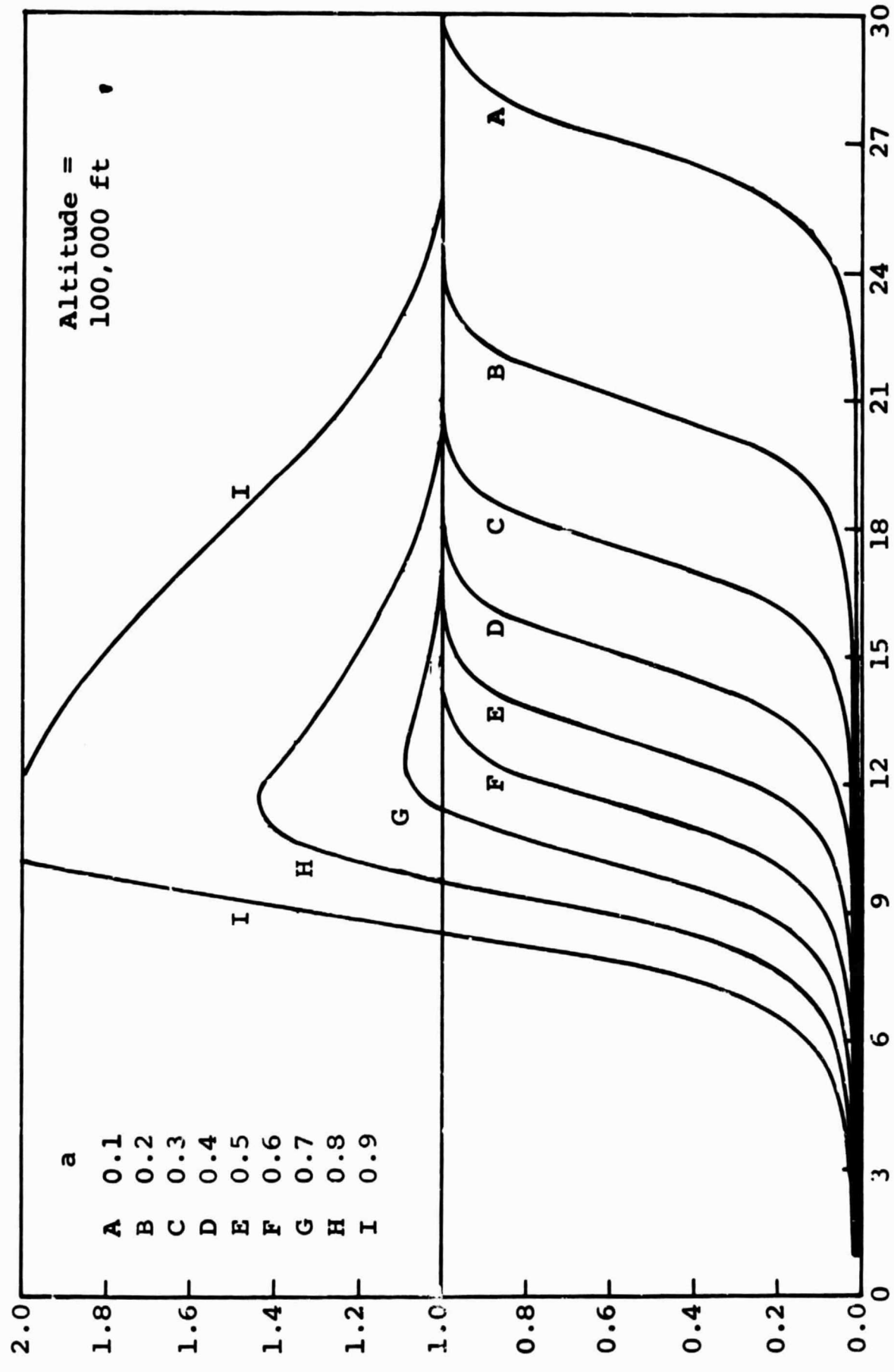

Fig. 21. Predicted performance with Rayleigh statistics at 100,000 ft.

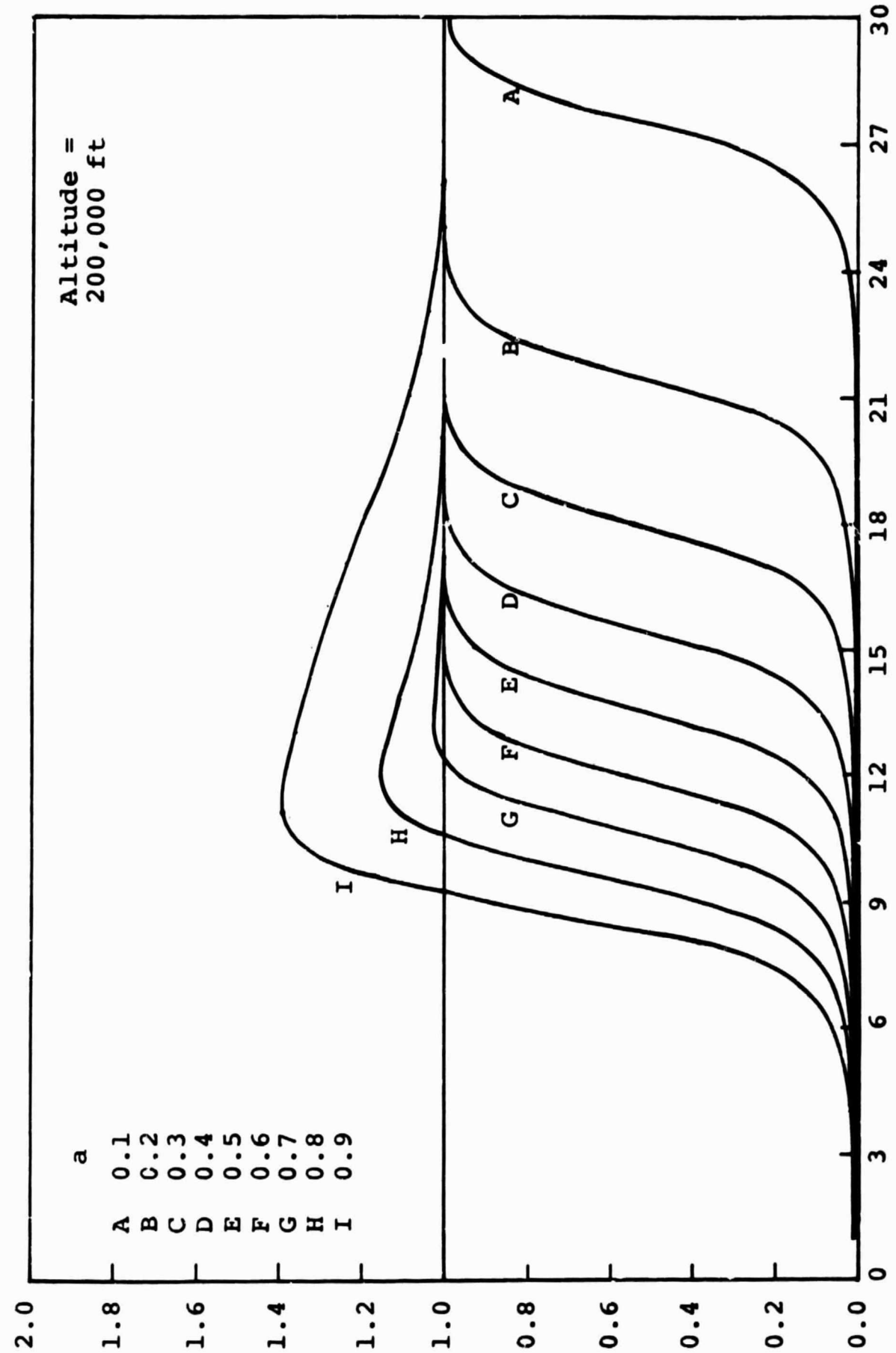

Fig. 22. Predicted performance with Rayleigh statistics at 200,000 ft.

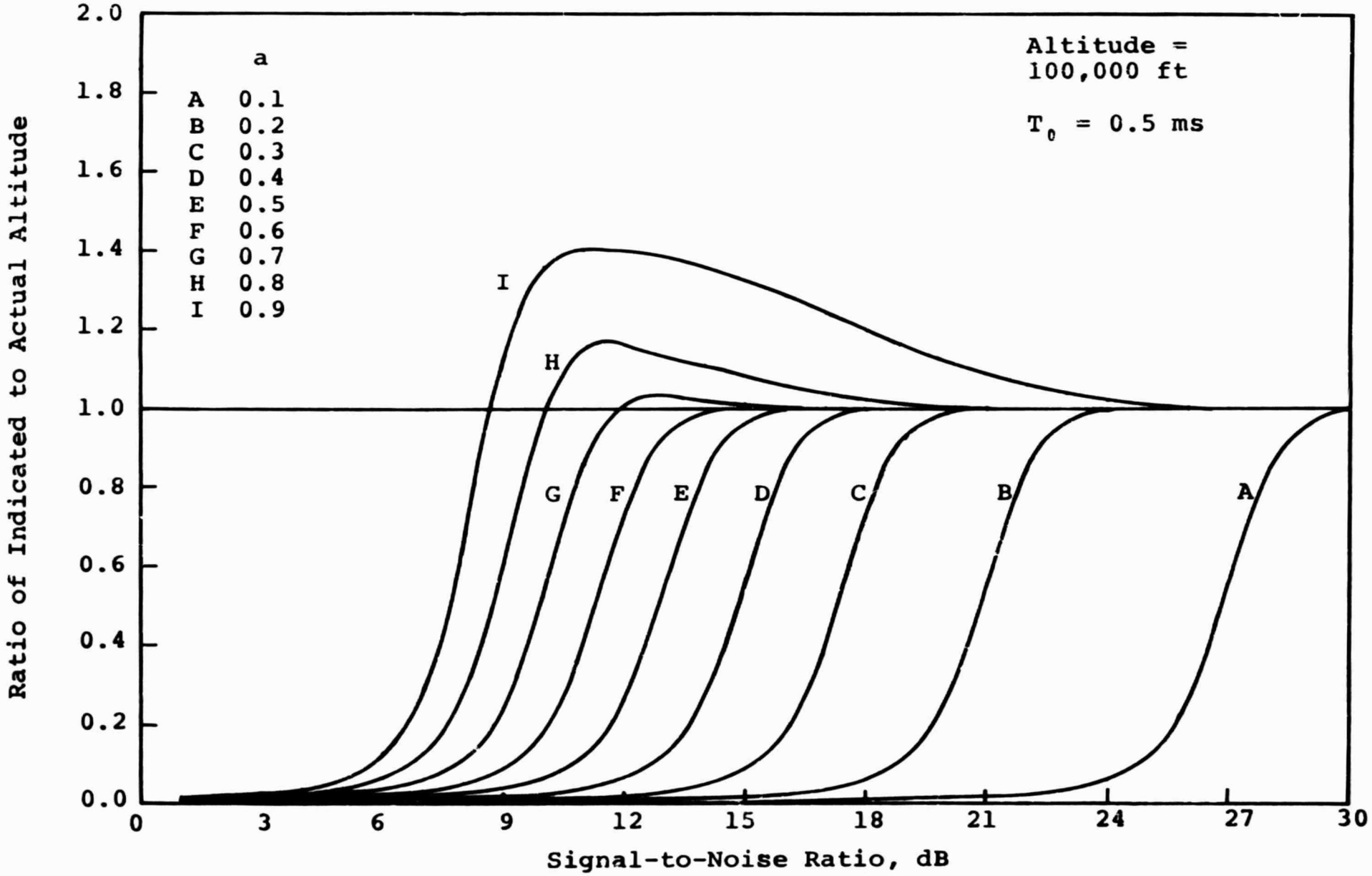

Fig. 23. Effects of changing the period with Rayleigh statistics at 100,000 ft.

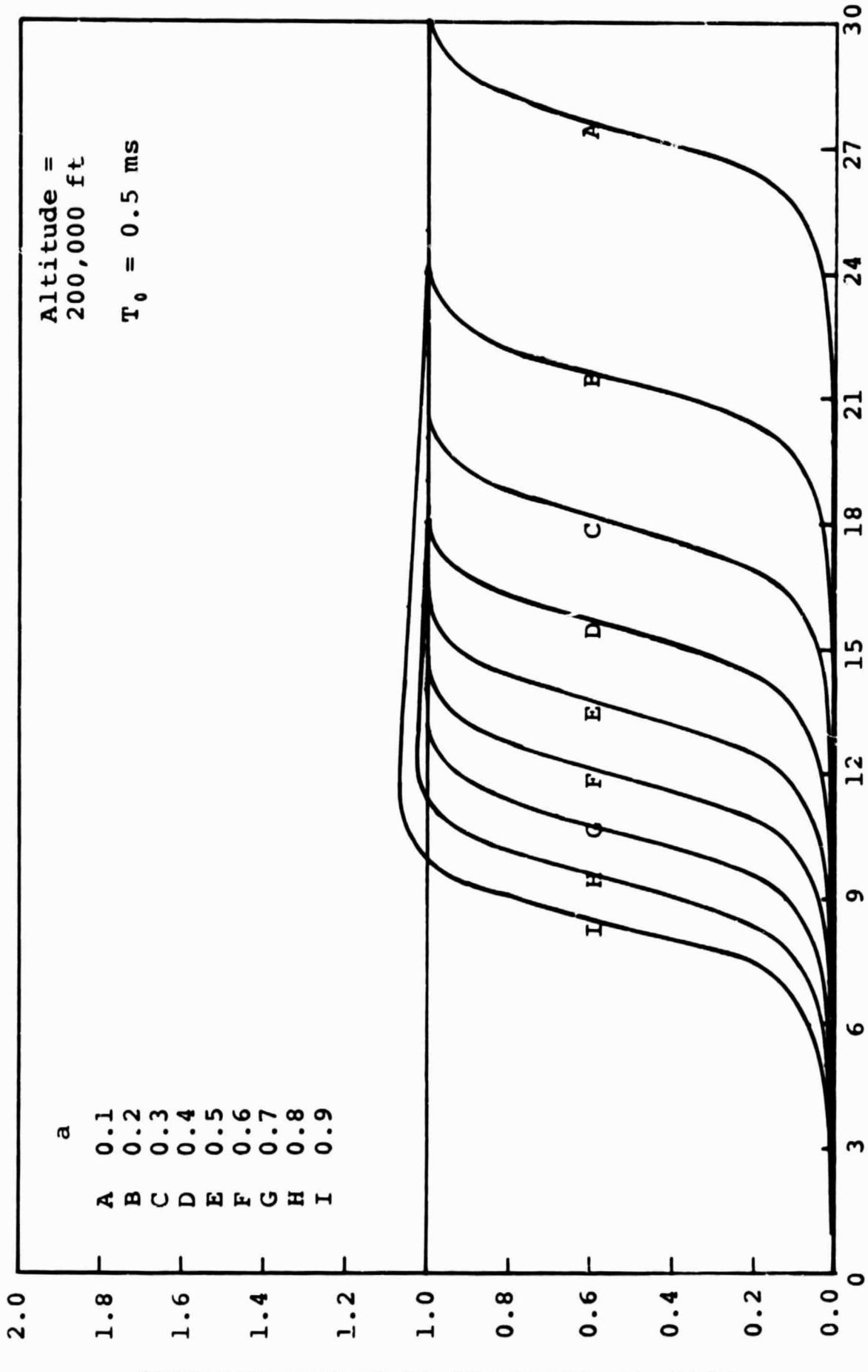

Fig. 24. Effects of changing the period with Rayleigh statistics at 200,000 ft.

END